



STUDIA UNIVERSITATIS  
BABEŞ-BOLYAI



# AMBIENTUM

---

1-2/2021

**STUDIA  
UNIVERSITATIS BABEȘ-BOLYAI  
AMBIENTUM**

**1-2 / 2021  
January – December**

**ISSUE DOI:10.24193/subbambientum.2021**

# STUDIA UNIVERSITATIS BABEȘ-BOLYAI AMBIENTUM

---

EDITORIAL OFFICE: 30, Fântânele Str., 400294 Cluj-Napoca, Phone: +40 264 307030

---

**Editor-in-Chief: Cristina ROȘU**

**Editors: Alexandru OZUNU, Călin BACIU, Liviu MUNTEAN,  
Radu MIHĂIESCU, Dumitru RISTOIU**

**Advisory Board:**

**Dan BĂLTEANU (Bucharest, Romania)  
Gheorghe DAMIAN (Baia-Mare, Romania)  
Giuseppe ETIOPE (Roma, Italy)  
Gabriel Ovidiu IANCU (Iasi, Romania)  
Adam MARKOWSKI (Lodz, Poland)  
Vasile OROS (Baia-Mare, Romania)  
Luis Santiago QUINDOS-PONCELA (Cantabria, Spain)  
Claude RONNEAU (Louvain la Neuve, Belgique)  
Carlos SAINZ-FERNANDEZ (Cantabria, Spain)  
Janos SOMLAI (Veszprem, Hungary)  
Shinji TOKONAMI (Chiba, Japan)  
Șerban Nicolae VLAD (Bucharest, Romania)**

**Editorial Secretary: Nicoleta BRIȘAN**

**Technical Secretaries: Ildiko MARTONOȘ  
Carmen ROBA**

**Cover 1: *Taxodium distichum* with *Tillandsia usneoides* (moss).  
Photo: Graeme Matthews**

<http://www.studia.ubbcluj.ro>

**YEAR  
MONTH  
ISSUE**

**Volume 66 (LXVI) 2021  
DECEMBER  
1-2**

---

**PUBLISHED ONLINE: 2022-10-30  
PUBLISHED PRINT: 2022-11-30  
ISSUE DOI: 10.24193/subbambientum.2021**

---

**S T U D I A  
UNIVERSITATIS BABEȘ-BOLYAI  
AMBIENTUM  
1-2**

---

**STUDIA UBB EDITORIAL OFFICE:** B.P. Hasdeu no. 51, 400371 Cluj-Napoca, Romania,  
Phone + 40 264 405352, office@studia.ubbcluj.ro

---

**CONTENTS – SOMMAIRE – CONTENIDO – CUPRINS**

- ANCA AVRAM, MARIUS MANDROC, DANIELA CONSTANTIN,  
SLOBODAN MARKOVIĆ, ALIDA TIMAR-GABOR – Optically  
stimulated luminescence dating of the upper horizon of a Serbian  
loess-paleosoil sequence using quartz ..... 5
- DAN FLORIN COSTIN – Chemical parameters of Bloaja Valley water  
affected by acid rock drainage, Băiuț mining area, Romania ..... 19
- ANGELA M. KASZA, GABRIEL KATONA, MONICA DAN, CEZARA  
VOICA, OANA GRAD, MARIA MIHEȚ, TIBOR DEZSO, RUBEN  
NAGY, TIHAMER BOTS, MIHAELA DIANA LAZĂR – Platinum  
recovery from used auto catalysts: dissolution and precipitation  
studies..... 33
- DORIN IOSIF MANCIULA, RADU BARBU HORAȚIU MIȘCA, ANDREI  
ROTAR – Polyurethane waste utilization ..... 45

GHEORGHE ROȘIAN, CSABA HORVATH, LIVIU MUNTEAN, NICOLAE BACIU – The influence of landform in the distribution of households of Ilva Mică territorial administrative unit .....	53
DIANA IULIANA TOMUȘ, CARMEN ROBA, CRISTINA ROȘU – Chemical characterisation of acid mine drainage from Valea Șesei tailing dam (NW of Romania) and its impact on surface water quality .....	63
MELINDA VIGH – The quantitative and qualitative parameters of the Bodoc springs .....	75

## OPTICALLY STIMULATED LUMINESCENCE DATING OF THE UPPER HORIZON OF A SERBIAN LOESS-PALEOSOIL SEQUENCE USING QUARTZ

**Anca AVRAM<sup>1,2,\*</sup>, Marius MANDROC<sup>1</sup>, Daniela CONSTANTIN<sup>1,2</sup>,  
Slobodan MARKOVIĆ<sup>3</sup>, Alida TIMAR-GABOR<sup>1,2</sup>**

<sup>1</sup>*Babeş-Bolyai University, Faculty of Environmental Science and Engineering,  
30 Fântânele Street, Cluj-Napoca, Romania*

<sup>2</sup>*Babeş-Bolyai University, Interdisciplinary Research Institute on Bio-Nano-Sciences,  
Environmental Radioactivity and Nuclear Dating Centre,  
Cluj-Napoca, Romania*

<sup>3</sup>*University of Novi, Sad Chair of Physical Geography, Faculty of Sciences, Serbia*

*\*Corresponding author: anca.avram92@gmail.com*

**ABSTRACT.** Optically stimulated luminescence dating is widely used for establishing high-resolution chronologies for the Quaternary in paleoclimate research. Loess is an important archive of past climate changes on continents. In order to provide a first absolute chronology for Zemun loess paleosol sequence in Serbia, the single-aliquot-regenerative dose (SAR) protocol was applied on coarse (63-90 µm) quartz fraction extracted from five samples. The profile reaches a thickness of 4 m, where the modern soil is visible in the uppermost part of the section. The investigated samples were collected from the transition between the uppermost visible soil and the loess layer, based on field observations. The results of the SAR-OSL protocol intrinsic rigor tests indicate that it can be successfully applied on coarse quartz extracted from Zemun samples, as all the results were within accepted limits of variation. The equivalent doses determined range from  $14 \pm 2$  Gy (ZMN 55A) to  $21 \pm 2$  Gy (ZMN 75A). Thus, the luminescence ages obtained for the investigated samples vary between  $5.4 \pm 0.7$  ka (ZMN 55A) and  $9.3 \pm 1.2$  ka (ZMN 75A). According to the ages obtained all the samples are assigned to the Holocene period.

**Key words:** *luminescence dating, quartz, loess, SAR protocol, OSL ages.*

## INTRODUCTION

The future environment trajectories may be predicted if the past conditions are very well known. Fortunately, the terrestrial surface of the Earth has the ability to preserve information about the past climatic conditions that guided the development of human species and their habitat. One of the most important terrestrial archives that were able to record the past climatic conditions is represented by loess deposits which are distributed over 10% of the world's continents and even more in some parts of Eurasia (Pécsi, 1990). Since loess-paleosol sequences are considered one of the most continuous and extensive terrestrial archives of the climate variability during Quaternary, they have a key role in assessing the landscape dynamics and global dust cycle (Schaetzl et al., 2018; Lehmkuhl et al., 2021). The specific characterisation of loess and paleosol alternations are related to climatic fluctuations. As such, loess units were formed during relatively dry-cool conditions whereas paleosol units were developed during a warm-humid period; all these are correlated with glacial-interglacial variability. In general, their timing is assumed to be simultaneous with the major climate changes that are very well documented in ice core and marine records (Bazin et al., 2013; Govin et al., 2015). In order to interpret the information recorded in these archives, the moment when the sediment was deposited should be assessed. Luminescence dating is an established method for this purpose. This technique uses minerals that are able to store charge upon irradiation in time. The energy accrued by the mineral due to natural occurring radioactivity can be released in the form of light and is represented by a signal in the form of a luminescence signal. This signal increases with the exposure to radioactivity in time and can be erased by exposure to light or heat. Since the first application of the Optically Stimulated Luminescence (OSL) dating on quartz (Huntley et al., 1985), technological improvements made during the last decades have contributed in significant developments on the accuracy and precision of this method. OSL dating using Single Aliquot Regenerative dose (SAR) protocol (Murray and Wintle 2000, 2003) is regarded as the most powerful dating methods that can establish absolute chronologies for loess deposits all over the world (e.g., Marković et al., 2014; Timar-Gabor et al., 2015; Constantin et al., 2014; Veres et al., 2018; Tecsca et al., 2020a, b; Avram et al., 2020, 2022; Brezeanu et al., 2021).

Loess-paleosol sequences in the Carpathian Basin in the form of dust deposition and soil formation during the Quaternary period, are known to provide information on the climatic variability in this region (Fuchs et al., 2008; Marković et al., 2008; Stevens et al., 2011). The province of Vojvodina is situated in the northern Serbia and represents a lowland part of the southern Carpathian Basin. This region encompasses the confluence area

of the Danube, Tisa and Sava rivers (Marković et al., 2008). Loess-paleosol sequences in the Vojvodina region are considered as one of the most extensive, complete and thickest terrestrial archives that were able to record past climatic events since the Pleistocene (Marković et al., 2015). OSL dating method has been successfully applied on several loess-paleosol sequences from Vojvodina region, such as: Stari Slankamen (Murray et al., 2014); Orlovat (Timar-Gabor et al., 2015); Mošorin (Constantin et al., 2019); Batajnica (Avram et al., 2020); Kisiljevo (Péřic et al., in press); Smederevo (Constantin et al., 2021).

The aim of this study is to assess the applicability of the OSL dating technique using the standard SAR protocol on quartz extracted from a loess deposit located in the Vojvodina region, Serbia, and to establish an absolute time frame for loess deposition using samples collected at the Pleistocene/Holocene transition as expected based on field observations.

## SAMPLING AND SITE DESCRIPTION

The loess profile (44° 51' 29" N and 20° 23' 13"E) investigated in this study (Zemun) is situated along the Danube in the Vojvodina region, in the north-western part of the outskirt of Belgrade in northern Serbia (figure 1). The sequence exhibits a thickness of approximately 4 m. Based on the field observations, the upper part of the profile with a thickness of 0.7 m represents the modern soil. At a depth of 50 cm, many krotovinas were observed.

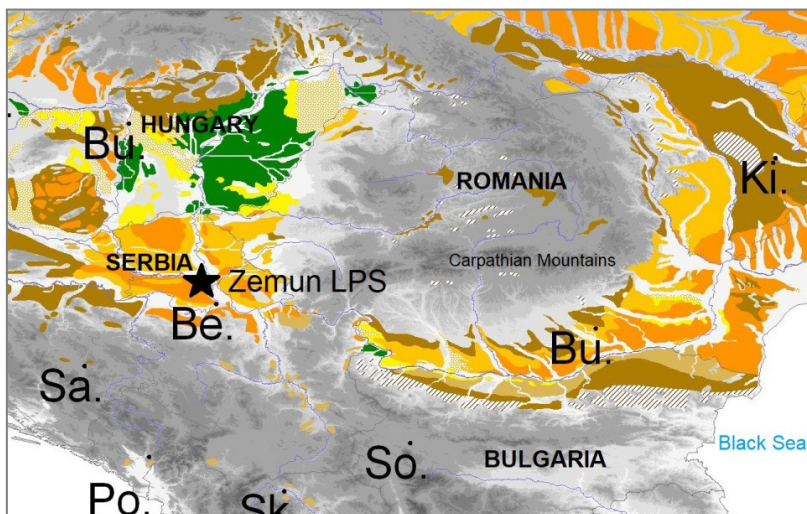


**Fig. 1.** The loess-paleosol sequence investigated in this study is represented by a star symbol and is integrated in the map of loess distribution (after Haase et al., 2007).

Since the upper part of the profile exposure allows investigating the Pleistocene/Holocene transition, the study site represents an important archive for dating the moment of the transition. Therefore, in the attempt to date the Pleistocene/Holocene transition, as recorded by field observations, five individual samples were collected and prepared for luminescence investigations. Based on the field observation, samples ZMN 55A and ZMN 65A were collected from the modern soil, denoted as S0, while ZMN 75A and ZMN 85A were sampled in order to match the transition. Moreover, a sample from L1 unit ZMN 95A was also collected.

## **OPTICALLY STIMULATED LUMINESCENCE DATING**

### **Sample preparation**

Five luminescence samples were collected in stainless steel tubes and prepared under subdued red light laboratory conditions. In order to avoid the contamination, the material from the end of each tube was removed and used for gamma spectrometry analysis. Quartz minerals were extracted from the material left in the inner part of the tube. First step of sample preparation consisted in a chemical treatment with hydrochloric acid of 10% concentration and hydrogen peroxide with a concentration of 30%, respectively. As a result, carbonates and organic matter were completely removed. Further, the sediment was separated into finer ( $<63 \mu\text{m}$ ) and coarser ( $>63 \mu\text{m}$ ) material through dry sieving. The grain size of interest ( $63\text{-}90 \mu\text{m}$ ) was obtained from the coarser material by sieving. Due to the small amount of coarse material, the density separation with heavy liquid could not be performed. To isolate quartz grains from the plagioclase feldspars, a prolong treatment with hydrofluoric acid (40% concentration for 1 hour) has been performed. To remove the precipitated fluorides, a rinse with hydrochloric acid (10% concentration) for 60 minutes has been carried out. In order to perform the luminescence measurements, the coarse quartz grains were mounted on stainless steel discs using silicon oil as an adhesive.

### **Analytical facilities**

Luminescence investigations were performed using two TL/OSL Risø DA-20 readers equipped with an automated detection and stimulation head (DASH) (Lapp et al., 2015). The intensity of the blue (470 nm) and infrared (870 nm) stimulation diodes are  $\sim 80$  and  $\sim 300 \text{ mW/cm}^2$ , respectively. Luminescence signal detection was made by using a PDM 9107Q-AO-TTL-

30 (160-630 nm) photomultiplier tube (Thomsen et al., 2006). Quartz signals were detected by 7.5-mm-thick Hoya U-340 UV filter. Laboratory irradiations were performed using the incorporated  $^{90}\text{Sr}$ - $^{90}\text{Y}$  radioactive sources that were calibrated with gamma-irradiated calibration quartz (Hansen et al., 2015). The dose rate of coarse quartz measured on the automated DASH reader was  $\sim 0.09$  Gy/s.

### Equivalent dose determination

Equivalent doses on coarse quartz were measured using a standard single aliquot regenerative dose (SAR) protocol (Murray and Wintle, 2000, 2003). The protocol is outlined in table 1. Blue-light emitting diodes were used for the optical stimulation which was carried out for 40 s at a temperature of 125 °C. In order to reduce the contribution of the slow and medium components, the net continuous wave optically stimulated luminescence (CW-OSL) signal of interest was integrated over the first 0.308 s of the decay curve minus an early background (Cunningham and Wallinga, 2010). Sensitivity change correction was made by using the OSL response to a test dose of 17 Gy. A preheat temperature of 220 °C for 10 s and a cutheat of 180 °C were employed. A high-temperature bleach (at 280 °C for 40 s) was performed at the end of each SAR cycle using blue diodes as stimulation source (Murray and Wintle, 2003).

In order to assess the robustness of the SAR protocol, the intrinsic performance tests (recycling and recuperation) (Murray and Wintle 2003) were integrated in every measurement. The purity of quartz luminescence signals was checked through the IR depletion test that consisted of adding an IR stimulation step prior to OSL measurement in the last cycle of the SAR protocol (Duller, 2003). Recycling and IR depletion ratios within 10% deviation from unity constituted the acceptance criteria for aliquots that were used in equivalent dose determination. Recuperation ratio was considered suitable if the value of the signal measured after a zero dose was less than 2% of the natural signal.

**Table 1.** Flowchart of the Single Aliquot Regenerative (SAR) dose protocol (Murray and Wintle 2000, 2003) applied in this study.

step	SAR protocol
1	Dose
2	Preheat (220 °C; 10s)
3	Blue OSL (125 °C; 40s)
4	Test dose (17Gy)
5	Cutheat (180 °C)
6	Blue OSL (125 °C; 40s)
7	Blue OSL (280 °C; 40s)

## Dosimetry

Radionuclide activity concentrations were determined by using a high-resolution gamma spectrometry. The measurements were carried out using a well-type HPGe detector. Samples were stored for one month in order to reach equilibrium between  $^{226}\text{Ra}$  and its parent  $^{222}\text{Rn}$ . The total dose rates were derived based on the conversion factors tabulated by Guérin et al. (2011). Based on the average humidity of loess samples in Vojvodina region, a time-average water content of 15% with an assumed relative error of 25% was used (e.g., Avram et al., 2020). A factor of 0.94 ( $\pm 5\%$  error) was assumed to correct the external beta dose rates for the effects of attenuation and etching (Mejdhal, 1979) and following the recommendation of Vandenberghe et al. (2008) an internal dose rate of  $0.010 \pm 0.002 \text{ Gy ka}^{-1}$  was adopted for the coarse fraction. The cosmic ray contribution to the total dose rate was calculated based on the formula tabulated by Prescott and Hutton (1994) using depth, altitude, latitude and longitude for each sample. Relevant information about the uranium, thorium and potassium concentration along with the cosmic dose rates are labelled in table 2 while the annual doses are displayed in table 3.

**Table 2.** *The specific radionuclide activities as well as the cosmic dose rates used for annual dose determination. It is assumed secular equilibrium between U and Ra. Specific activities were measured using high-resolution gamma spectrometry.*

Sample code	Specific activities (Bq/kg)			Cosmic dose rate
	K-40	Th-232	Ra-226	
ZMN 55A	370 $\pm$ 12	38 $\pm$ 2	42 $\pm$ 3	0.212 $\pm$ 0.032
ZMN 65A	324 $\pm$ 10	38 $\pm$ 3	37 $\pm$ 1	0.206 $\pm$ 0.031
ZMN 75A	301 $\pm$ 10	34 $\pm$ 3	36 $\pm$ 1	0.201 $\pm$ 0.030
ZMN 85A	374 $\pm$ 14	36 $\pm$ 3	35 $\pm$ 2	0.197 $\pm$ 0.030
ZMN 95A	369 $\pm$ 11	31 $\pm$ 3	27 $\pm$ 2	0.193 $\pm$ 0.029

## RESULTS AND DISCUSSIONS

### Luminescence properties of quartz

The net signals of coarse quartz decay significantly within the first seconds of optical stimulation as documented for sample ZMN 55A in the inset of figure 2. The pattern exhibited by the natural and regenerated decay curves of coarse quartz appear indistinguishable with that measured for calibration quartz, which is accepted to be dominated by the fast component (Hansen et al., 2015).

OPTICALLY STIMULATED LUMINESCENCE DATING OF THE UPPER HORIZON OF A SERBIAN LOESS-PALEOSOIL SEQUENCE USING QUARTZ

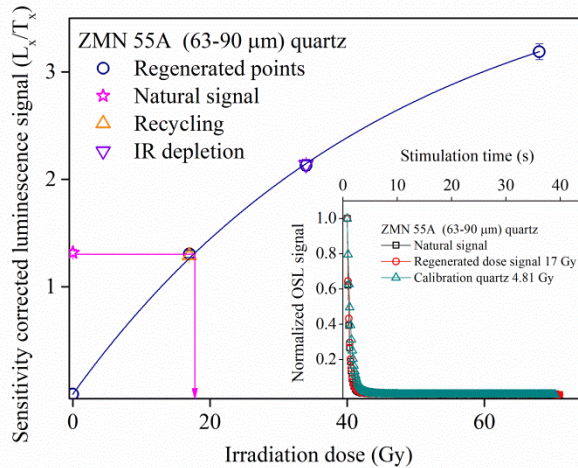


**Fig. 2.** Representative sensitivity-corrected dose response curve constructed for sample ZMN 55A using one aliquot of coarse quartz. The sensitivity corrected natural signal (star symbol) is interpolated on the dose response curve. IR depletion point is presented as an inverse triangle while Recycling point is depicted by an up triangle. The inset shows the pattern of a typical quartz decay curve which is compared with the decay of a regenerative dose as well as with the OSL decay of calibration quartz.

Representative SAR laboratory growth curve constructed for a single aliquot of 63-90  $\mu\text{m}$  quartz from sample ZMN 55A is displayed in figure 2. The dose response curves were well described by a sum of two saturating exponential function. Ratios within 10% from unity were obtained for recycling and IR depletion ratios. These results demonstrate that the sensitivity changes during the repeated SAR cycles are properly corrected for, and that the investigated signals come from quartz and no other contaminant minerals.

### Dose recovery test

The single and most complete test that characterise the performance of the SAR procedure for any given sample is the dose recovery test (Murray and Wintle 2003). It is used to assess whether the SAR protocol can accurately measure a known dose administered prior to any thermal treatment. Sets of five aliquots of 63-90  $\mu\text{m}$  quartz from samples ZMN 55A and ZMN 95A were used. The natural signals were first removed by a double exposure to blue light emitting diodes for 100 s at room temperature with a pause of 10 ks. Further, the aliquots were irradiated with laboratory beta doses chosen to be similar to equivalent doses. The given dose is then measured using the SAR

protocol in the same manner as the equivalent doses. The dose recovery ratio was further calculated by dividing the recovered to the given dose. The value of the dose recovery ratio should be close to unity. The results of the dose recovery test are presented in Figure 3. As can be seen, for sample ZMN 55A, a dose recovery ratio of  $0.95\pm 0.02$  was calculated whereas for sample ZMN 95 A, a ratio of  $0.97\pm 0.02$  was obtained. These results suggested that the SAR protocol can successfully measure the doses over the interval investigated here.

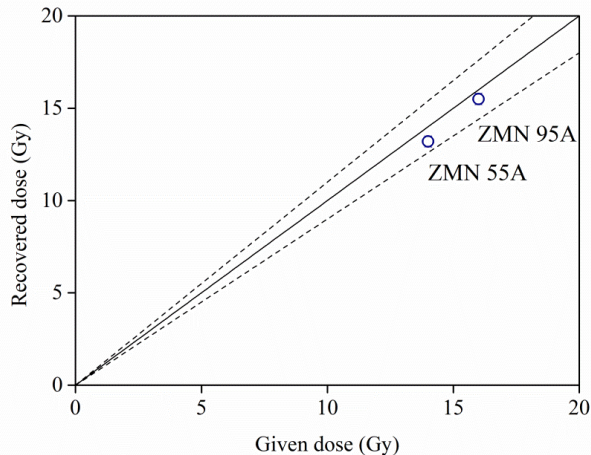


**Fig. 3.** Dose recovery test results for 63-90  $\mu\text{m}$  quartz using SAR protocol. The given irradiation doses were chosen to be similar with the equivalent dose for each sample. The solid line indicates the ideal 1:1 dose recovery ratio while dashed lines indicate a 10% variation from unity.

### Equivalent doses

Equivalent doses were determined by projecting the sensitivity corrected natural luminescence signal onto the dose response curve constructed for each sample investigated (Figure 2). 10 replicate measurements were carried out for each sample in order to calculate the equivalent dose. Table 3 summarises the measured equivalent dose for each sample as well as the results of the intrinsic tests of the SAR protocol (Recycling, IR depletion and Recuperation). The obtained equivalent doses range from  $14\pm 2$  Gy for sample ZMN 55A to  $21\pm 2$  Gy for sample ZMN 75A.

### Luminescence ages

OSL ages are represented in table 3 and figure 4 as function of depth. As can be seen, for the uppermost sample collected from a depth of 55 cm

an age of  $5.5 \pm 0.7$  ka (ZMN 55A) was obtained, whereas for the sample collected from a depth of 95 cm an age of  $7.4 \pm 1.0$  ka (ZMN 95A) was calculated. In this depth interval of sample collection, the oldest age ( $9.3 \pm 1.2$  ka) was obtained for sample ZMN 75A. As can be seen, the ages are increasing with depth up to sample ZMN 75A while for samples ZMN 85 A and ZMN 95 A the ages are smaller. The age inversion is often encountered in the upper parts of loess-paleosol profiles and it is considered to be the effect of the paedogenetic process (e.g., Constantin et al., 2021).

**Table 3.** Summary of the SAR-OSL ages. The age uncertainties were determined following **Aitken and Ailred (1972)**. The uncertainties associated with the luminescence and dosimetry data are random; the uncertainties mentioned on the optical ages are the overall uncertainties. The ages were calculated considering  $15 \pm 4\%$  water content.

Sample code	Depth (cm)	Equivalent dose (Gy)	Total dose rate (Gy/ka)	Age (ka)
ZMN 55A	55	$14 \pm 2$	$2.6 \pm 0.06$	$5.4 \pm 0.7$
ZMN 65A	65	$16 \pm 2$	$2.3 \pm 0.04$	$6.8 \pm 0.9$
ZMN 75A	75	$21 \pm 2$	$2.2 \pm 0.06$	$9.3 \pm 1.2$
ZMN 85A	85	$20 \pm 3$	$2.4 \pm 0.07$	$8.4 \pm 1.4$
ZMN 95A	95	$16 \pm 2$	$2.2 \pm 0.06$	$7.4 \pm 1.0$

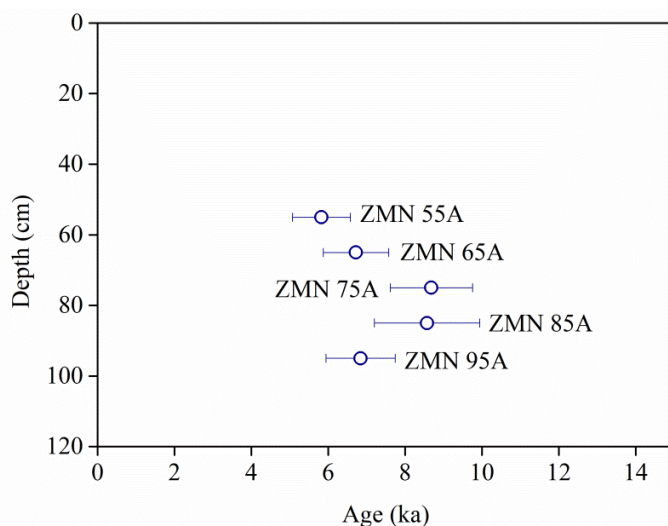


**Fig. 4.** Luminescence ages obtained on coarse quartz extracted from Zemun samples plotted as function of depth.

## **DISCUSSION AND CONCLUSIONS**

As far as methodological dating investigations are concerned, Optically Stimulated Luminescence dating has been successfully applied on quartz samples investigated in this study. The sensitivity corrected luminescence signal of 63-90  $\mu\text{m}$  quartz was shown to be dominated by the fast component and thus exhibiting the optimal characteristics for the application of the SAR protocol. The robustness of the applied protocol has been assessed through the intrinsic tests, namely: Recycling, Recuperation and IR depletion test. The results of these tests were within the acceptability criteria, demonstrating the robustness of the protocol.

The aim of this study was to provide absolute luminescence ages for 5 loess samples collected from Zemun loess sequence located in Vojvodina region in order to establish the moment of the Pleistocene/Holocene transition as assigned by field observations only. For the samples collected in this regard, the OSL ages increase up to an age of  $9.3 \pm 1.2$  ka obtained for sample ZMN 75A. This sample was thought to be collected exactly from the depth where the Pleistocene/Holocene transition was identified in the field. The timing of the Pleistocene/Holocene boundary defined in ice-core records is 11.7 ka (Rasmussen et al., 2014; Walker et al., 2019). A recent study conducted by Constantin et al. (2021) investigated the moment of Pleistocene/Holocene transition as recorded by variations of the magnetic susceptibility in loess worldwide, concluding that the timing of the Pleistocene-Holocene climatic transition, as recorded by this proxy is prior to 11.7 ka, around 14-17.5 ka. Our results show a mismatch between the chronological information obtained by luminescence dating and the field information collected during the sampling. As such, for this particular section our results highlight the need for dating more samples collected at larger depths as well as the necessity of carrying out magnetic susceptibility measurements. Overall, this study demonstrated that stratigraphic boundaries and their associated climatic transitions cannot be accurately identified in loess-paleosoil sequences based on field observations only, highlighting the need for using proxies and the application of absolute dating methods.

### **Acknowledgements**

This study was funded by the European Research Council (ERC) under the European Union's Horizon 2020 research and innovation programme ERC-2015-STG, (grant agreement No [678106]).

Anca Avram and Alida Timar-Gabor received financial support of the research project EEA-RO-NO-2018-0126.

## REFERENCES

- Aitken M. J., Alldred J. C., 1972, The assessment of error limits in thermoluminescent dating. *Archaeometry* **14**, pp. 257–267.
- Avram A., Constantin D., Veres D., Kelemen S., Obrecht I., Hambach U., Marković S. B., Timar-Gabor A., 2020, Testing polymineral post-IR IRSL and quartz SAR-OSL protocols on Middle to Late Pleistocene loess at Batajnica, Serbia. *Boreas*, **49**, pp. 615–633.
- Avram A., Constantin D., Hao Q., Timar-Gabor A., 2022, Optically stimulated luminescence dating of loess in South-Eastern China using quartz and polymineral fine grains. *Quat. Geochronol.* **67**, pp. 101226.
- Bazin L., Landais A., Lemieux-Dudon B., Toyé Mahamadou Kele H., Veres D., Parrenin F., Martinerie P., Ritz C., Capron E., Lipenkov V., Loutre M. F., Raynaud D., Vinther B., Svensson A., Rasmussen S., Severi M., Blunier T., Leuenberger M., Fischer H., Masson-Delmotte V., Chappellaz J., Wolff E., 2013, An optimized multi-proxy, multi-site Antarctic ice and gas orbital chronology (AICC2012): 120-800 ka. *Clim. Past*, **9**, pp. 1715–1731.
- Brezeanu D., Avram A., Micallef A., Cinta Pinzaru S., Timar-Gabor A., 2021, Investigations on the luminescence properties of quartz and feldspars extracted from loess in the Canterbury Plains, New Zealand South Island. *Geochronometria*, **48**, pp. 46-60.
- Constantin D., Begy R., Vasiliu S., Panaiotu C., Necula C., Codrea V., Timar-Gabor A., 2014, High-resolution OSL dating of the Costinesti section (Dobrogea SE Romania) using fine and coarse quartz. *Quat. Int.*, **334-335**, pp. 20-29.
- Constantin D., Veres D., Panaiotu C., Anechitei-Deacu V., Groza S. M., Begy R. C., Kelemen S., Buylaert J. P., Hambach U., Marković S. B., Gerasimenko N., Timar-Gabor A., 2019, Luminescence age constraints on the Pleistocene-Holocene transition recorded in loess sequences across SE Europe. *Quat. Geochronol.*, **49**, pp. 71–77.
- Constantin D., Mason J. A., Veres D., Hambach U., Panaiotu C., Zeeden C., Zhou L., Marković S.B., Gerasimenko N., Avram A., Tecsa V., Groza-Sacaciu S. M., del Valle Villalonga L., Begy R., Timar-Gabor A., 2021, *Earth-Sci. Rev.*, **221**, pp. 103769.
- Cunningham A. C., Wallinga J., 2010, Selection of integration time intervals for quartz OSL decay curves. *Quat. Geochronol.*, **5**, pp. 657–666.
- Duller G. A. T., 2003, Distinguishing quartz and feldspars in single grain luminescence measurements. *Radiat. Meas.*, **37**, pp. 161–165.
- Fuchs M., Rousseau D. D., Antoine P., Hatté C., Gauthier C., Marković S. B., Zoeller L., 2008, High resolution chronology of the upper Pleistocene loess/paleosol sequence at Surduk, Vojvodina, Serbia. *Boreas*, **37**, pp. 66–73.

- Govin A., Capron E., Tzedakis P.C., Verheyden S., Ghaleb B., Hillaire-Marcel C., St-Onge G., Stoner J. S., Bassinot F., Bazin L., Blunier T., Combourieu-Nebout N., El Ouahabi A., Genty D., Gersonde R., Jimenez-Amat P., Landais A., Martrat B., Masson-Delmotte V., Parrenin F., Seidenkrantz M.-S., Veres D., Waelbroeck C., Zahn R., 2015, Sequence of events from the onset to the demise of the last Interglacial: evaluating strengths and limitations of chronologies used in climatic archives. *Quat. Sci. Rev.*, **129**, pp. 1–36.
- Guérin G., Mercier N., Adamiec G., 2011, Dose-rate conversion factors: update. *Ancient TL*, **29**, pp. 5–8.
- Haase D., Fink J., Haase G., Ruske R., Pécsi M., Richter H., Altermann M., Jager K. D., 2007, Loess in Europe - its spatial distribution based on a European Loess Map, scale 1:2,500,000. *Quat. Sci. Rev.*, **26**, pp. 1301–1312.
- Hansen V., Murray A., Buylaert J. P., Yeo E. Y., Thomsen K., 2015, A new irradiated quartz for beta source calibration. *Radiat. Meas.*, **81**, pp. 123–127.
- Huntley D. J., Godfrey-Smith, D. I., Thewalt M. L. W., 1985, Optical dating of sediments. *Nature*, **313**, pp. 105–107.
- Lapp T, Kook M, Murray A. S., Thomsen K. J., Buylaert J. P., Jain M., 2015, A new luminescence detection and stimulation head for the Risø TL/OSL reader. *Radiation Measurements*, **81**, pp. 178–184,
- Lehmkuhl F., Nett J. J., Pötter S., Schulte P., Sprafke T., Jary Z., Antoine P., Wacha L., Wolf D., Zerboni A., Hösek J., Marković S. B., Obrecht I., Sümegi P., Veres D., Zeeden C., Boemke B., Schaubert V., Viehweger J., Hambach U., 2021, Loess landscapes of Europe—Mapping, geomorphology, and zonal differentiation. *Earth Sci. Rev.* 103496.
- Marković SB, Bokhorst MP, Vandenberghe J, et al. 2008. Late Pleistocene loess–paleosol sequences in the Vojvodina region, north Serbia. *Journal of Quaternary Science*, **23**, 73–84.
- Marković S. B., Timar-Gabor A., Stevens T., Hambach U., Popov D., Tomić N., Obrecht I., Jovanović M., Lehmkuhl F., Kels H., Marković R., Gavrilov M. B., 2014, Environmental dynamics and luminescence chronology from the Orlovat loess-paleosol sequence (Vojvodina, northern Serbia). *J. Quat. Sci.*, **29**, pp. 189–199.
- Marković S. B., Stevens T., Kukla G. J., Hambach U., Fitzsimmons K., Gibbard P., Buggle B., Zech M., Guo Z., Hao Q., Wu H., O’Hara-Dhand K., Smalley I., Ujvari G., Sümegi P., Timar-Gabor A., Veres D., Sirocko F., Vasiljevic D., Svircev Z., 2015, Danube loess stratigraphy – Towards a pan-European loess stratigraphic model. *Earth-Sci. Rev.*, **148**, pp. 228–258.
- Mejdahl V., 1979, Thermoluminescence dating: beta-dose attenuation in quartz grains. *Archaeometry*, **21**, pp. 61–72.
- Murray A. S., Wintle A. G., 2000, Luminescence dating using an improved single-aliquot regenerative-dose protocol. *Radiat. Meas.*, **32**, pp. 57–73.
- Murray A. S., Wintle A.G., 2003, The single aliquot regenerative dose protocol: potential for improvements in reliability. *Radiat. Meas.*, **37**, pp. 377–381.

- Murray A. S., Schmidt E. D., Stevens T., Buylaert J.-P., Marković S. B., Tsukamoto S., Frechen M., 2014, Dating Middle Pleistocene loess from Stari Slankamen (Vojvodina, Serbia) – Limitations imposed by the saturation behaviour of an elevated temperature IRSL signal. *Catena*, **117**, pp. 34–42.
- Pécsi M., 1990, Loess is not just the accumulation of dust. *Quat. Int.*, **7-8**, pp. 1-21.
- Perić Z. M., Marković S. B., Avram A., Timar-Gabor A., Zeeden C., Nett J. J., Fischer P., Fitzsimmons K. E., Gavrilov M. B., *Quat. Int.*, in press., <http://dx.doi.org/10.1016/j.quaint.2020.10.040>.
- Prescott J. R., Hutton J. T., 1994, Cosmic ray contributions to dose rates for luminescence and ESR dating: large depths and long term variations. *Radiat. Meas.*, **23**, pp. 497–500.
- Rasmussen S. O., Bigler M., Blockley S. P., Blunier T., Buchardt S. L., Clausen H. B., Cvijanovic I., Dahl-Jensen D., Johnsen S. J., Fischer H., Gkinis V., Guillevic M., Hoek W. Z., Lowe J. J., Pedro J. B., Popp T., Seierstad I. K., Steffensen J. P., Svensson A. M., Vallelonga P., Vinther B. M., Walker M. J. C., Wheatley J. J., Winstrup M., 2014. A stratigraphic framework for abrupt climatic changes during the last Glacial period based on three synchronized Greenland ice-core records: refining and extending the INTIMATE event stratigraphy. *Quat. Sci. Rev.*, **106**, pp. 14–28.
- Schaetzl R. J., Bettis E. A., Crouvic O., Fitzsimmons K. E., Grimley D. A., Hambach U., Lehmkuhl F., Marković S. B., Mason J. A., Owczarek P., Roberts H. M., Rousseau D. D., Stevens T., Vandenberghe J., Zarate M., Veres D., Yang S. L., Zech M., Conroy J. L., Dave A. K., Faust D., Hao Q. Z., Obrecht I., Prud'homme C., Smalley I., Tripaldi A., Zeeden C., Zech R., 2018, Approaches and challenges to the study of loess - introduction to the Loess-Fest. *Quat. Res.*, **89**, pp. 563–618.
- Stevens T., Marković S. B., Zech M., Hambach U., Sümegi P., 2011, Dust deposition and climate in the Carpathian Basin over an independently dated last glacial–interglacial cycle. *Quat. Sci. Rev.*, **30**, pp. 662–681.
- Tecsa V., Gerasimenko N., Veres D., Hambach U., Lehmkuhl F., Schulte P., Timar-Gabor A., 2020a, Revisiting the chronostratigraphy of late Pleistocene loess-paleosol sequences in southwestern Ukraine: OSL dating of Kurortnesection. *Quat. Int.*, **542**, pp. 65–79.
- Tecsa V., Mason J.A., Johnson W.C., Miao X., Constantin D., Radu S., Magdas D.A., Veres D., Marković S. B., Timar-Gabor A., 2020b, Late Pleistocene to Holocene loess in the central Great Plains: Optically stimulated luminescence dating and multi-proxy analysis of the Enders section (Nebraska, USA). *Quat. Sci. Rev.*, **229**, pp. 106130.
- Thomsen K. J., Bøtter-Jensen L., Denby P. M., Moska P., Murray A. S., 2006, Developments in luminescence measurement techniques. *Radiat. Meas.*, **41**, pp. 768–773.
- Timar-Gabor A., Constantin D., Marković S. B., Jain M., 2015, Extending the area of investigation of fine versus coarse quartz optical ages from the Lower Danube to the Carpathian Basin. *Quat. Int.*, **388**, pp. 168-176.

- Vandenberghé D. A. G., De Corte F., Buylaert J.-P., Küçera J., Van den Haute P., 2008, On the internal radioactivity in quartz. *Radiat. Meas.*, **43**, pp. 771–775.
- Veres D., Tecsá V., Gerasimenko N., Zeeden C., Hambach U., Timar-Gabor A., 2018, Short-term soil formation events in last glacial east European loess, evidence from multi-method luminescence dating. *Quat. Sci. Rev.*, **200**, pp. 34–51.
- Walker M., Head M. J., Lowe J., Berkelhammer M., Björck S., Cheng H., Cwynar L., Fisher D., Gkinis V., Long A., Lowe J., Newnham R., Rasmussen S., Weiss H., 2019, Subdividing the Holocene Series/Epoch: formalization of stages/ages and subseries/subepochs, and designation of GSSPs and auxiliary stratotypes. *J. Quat. Sci.*, **34**, pp. 173–186.

# CHEMICAL PARAMETERS OF BLOAJA VALLEY WATER AFFECTED BY ACID ROCK DRAINAGE, BĂIUȚ MINING AREA, ROMANIA

Dan Florin COSTIN<sup>1\*</sup>

<sup>1</sup>*Babeş-Bolyai University, Faculty of Environmental Science and Engineering,  
30 Fântânele Street, 400294, Cluj-Napoca, Romania*

*\*Corresponding author: dan.costin@ubbcluj.ro*

**ABSTRACT.** Mining areas are among the most polluted industrial sites, the surface waters being often affected by acid rock drainage. Mine and processing wastes represents one of the main sources of acidic waters. The seepages from Bloaja tailings management facilities have a low pH and increased total dissolved solids. Chemical analyses show high Zn, Cu and Pb concentrations of the contact water with the pyrite concentrate deposited on Bloaja Old tailings management facility. These polluted waters are discharged in the watercourses, decreasing the quality of surface water. Despite of the remediation of Bloaja New tailings management facility, the waste waters seepages have a conspicuous environmental impact on watercourses from Lăpuş River basin.

**Key words:** *mining area, tailings, acid rock drainage, pyrite concentrate, heavy metals, water pollution.*

## INTRODUCTION

The development of human society through history is strongly associated with complex materials made from mineral resources. Mining is one of the most polluting industries, with serious effects on human health (Candeias et al., 2018). In mining regions, the risks related to the management of mine wastes and tailings are very high both in the operational phase and in the post-closure time (Kossoff et al., 2014). A difficult environmental issue occurring in mining regions is acid rock drainage characterized by elevated metals concentrations of underground and surface waters (Nordstrom, 2011).

Finding a control and/or treatment strategy of these phenomenon for a certain mining region is a complex task due to the diversity of factors on which the formation depends (Skousen et al., 2019). The geochemical background of the studied area is important in order to assess the contribution of acid rock drainage to the water chemistry (Matschullat et al., 2000).

The century-old mining of the non-ferrous metals ore deposits in Baia Mare region, one of the most famous mining region from Romania, has led to a heavy legacy for all environmental components: air, water and soil. Some heavy metals pollution problems have been attenuated by the closing of mining activities which begins in 2006 and by some rehabilitations measures implemented on the most severely affected areas. However, the management the waters affected by the acid rock drainage has not been addressed properly in order to minimize the associated risks (Costin and Baciu, 2010).

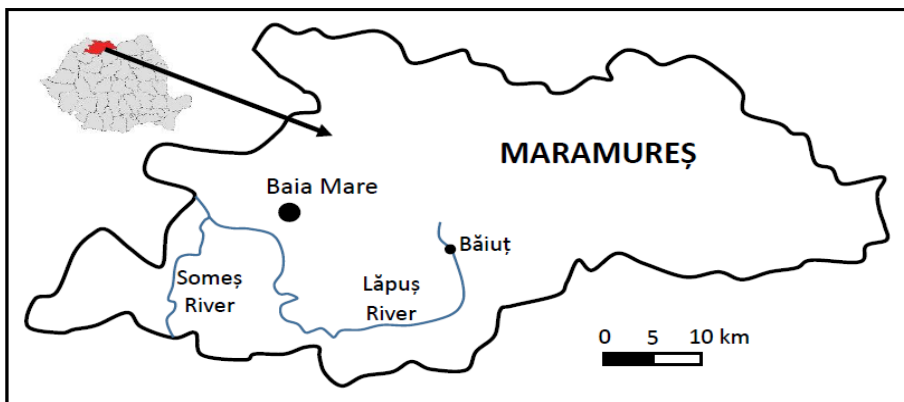


**Fig. 1.** Location of Băiuț mining area in Maramureș County

This paper is focused on some aspects of environmental impact of processing wastes from Băiuț mining area, a mining district of Baia Mare region. The aim of this study is to evaluate the consequences of the acid rock drainage discharged from Bloaja Valley tailings management facilities on the chemistry of surface waters in order to facilitate the finding of better remediation methods.

## **STUDY AREA**

Băiuț area is located at 80 km south-east of Baia Mare city, in easternmost part of Oaș-Gutâi-Țibleș volcanic mountains, geographical unit

belonging to East Carpathians (figure 1). Considering the values of the landscape fragmentation density and the maximum elevations, this area has sub-mountain characteristics. Lăpuș River springs from this region and downstream it collects a relative large number of small creeks forming the main watercourse of the Lăpuș sedimentary basin. The landscape formation was strongly influenced by the complex geological structure.

A geological succession of Mesozoic, Paleogene and Neogene sedimentary formation (clays, marls, sandstone and limestone) was partially covered by volcanoclastics and volcanic rocks (mainly andesite) and pierced by subvolcanic bodies (Aroldi, 2001). Associated with volcanic activity, a metallogenetic episode has generated ore deposits (Borcoș and Gheorghită, 1976). Veins are the main orebody type of these deposits, having a polymetallic character (lead, zinc, copper) with significant amounts of precious metals (gold and silver). The geological and geochemical characteristics of the ore deposits define its assignment to the epithermal type (Costin, 2000; Costin and Vlad, 2005).

The valorization of mineral resources has a long tradition in Băiuț area, the first mining activities being carry out in the Middle Age time (Achim and Ciolte, 1991). The awareness of environmental problems associated with mining has begun to emerge in the last few decades. The main sources of acid rock drainage are the discharged waters from the closed underground works and in conservation tailings management facilities. Băiuț area is considered one of the most important pollution point in the north-western Romania (Bird et al, 2003). Some preliminary data were presented by Costin and Marina (2006) and Costin (2007) regarding the pollution associated with acid rock drainage occurring in one of the ore extraction field. Detailed studies were conducted in Băiuț area in order to assess the heavy metals pollution effects on the soil quality (Chira et al., 2014; Doroțan et al., 2015; Doroțan et al., 2018). Maramureș County Committee for Emergency Situations (2016) included Băiuț area on the list of the main areas of the Maramureș County potentially generating pollution on watercourses due to the existence of the closed mine facilities and mine wastes.

Bloaja Valley belongs to the upper basin of Lăpuș River. This typical mountain v-shape valley with a length of approx. 3 km is a left tributary of Lăpuș River. Two tailings management facilities (TMF) were built up in this area: Bloaja New cross-valley type tailings impoundment and Bloaja Old side-hill type tailings impoundment. The area is located at 7 km downstream of the former flotation plant.

Bloaja New TMF has an area of 15.30 ha, a length of 525 m, an average width of 217 m, and a capacity of 2.46 million m<sup>3</sup>. Due to the small slope of the natural terrain (1.2%), two dams were gradually raised in order

to create the necessary space to tailings deposition in the pond: a smaller upstream dam and a larger downstream dam. The height of the downstream dam is 44.50 m. Upstream of the TMF, the diversion of Bloaja Valley was made through a visiting canal with a length of 517 m, built of reinforced concrete. In the extension of the canal, a tunnel with a length of 243 m was excavated in the slope hill on the left side of the valley.

In the operational phase, the freewater from the pond that resulted after the tailings sedimentation was evacuated by three decant wells connected to a pipe laid on the bed of the TMF. The surface water runoff which passes through the upstream tailings dam is released at the base of the dam diffusely forming a swampy area. Drain pipes were installed at the bottom of the downstream dam in order to control the seepage outflow. The collected water is spilled into Bloaja Valley, downstream of the tunnel.

The commissioning of the pond was carried out in 1975 and it was operational until 2007 when Băiș mine was closed. During this time, there were no damages that would endanger the stability of the pond and the safety of its operation. In the post-closure period, a reclamation and ecological rehabilitation program has been carried out on the surface of the pond and the two dams. The main objectives of the works were to control the runoff and erosion, the infiltration, and the seepage. After the compaction and levelling of the tailings, the surface of the TMF was covered with geomembrane. Geotextile materials added on top of this impermeable level provided the foundation of the topsoil which has been cultivated with local vegetation. On the reclaimed TMF, a surface water diversion system composed by a network of concrete channels has been installed. A complex system of drains linked to the surface water channels is used to manage the seepages. There is no water treatment facility downstream of the reclaimed TMF

Located at 450 m SW from Bloaja New TMF, was in operation between 1972 and 1975. After its closure, initially these impoundments were managed as an emergency facility in case of unforeseen events that would occur at the deposition to the tailings in the new TMF. Due to the short time of operational phase, a small amount of tailings was deposited (approximately 91,000 m<sup>3</sup>) on a surface area of 5.20 ha. The height of the dam is 10 m. Later, a concrete wall was built on the northern and western sides of Bloaja Old TMF to store the pyrite concentrate which could not be marketed as piles. No maintenance and remediation works were done on this TMF. Rills and gullies are created by the surface water that runoffs freely over the concentrate and the tailings, transporting these mineral materials outside the TMF and covering large areas of flat terrain in the nearby. The contact water forms small pool on the surface of the TMF or it is collected in a small channel made on the bottom of the dam from where it is discharged into Bloaja Valley.

## SAMPLING AND ANALYTICAL METHOD

In order to evaluate the quality of the surface water in the area of the two TMF, a sampling network with ten points was chosen. The location and the description of the sampling points are presented in figure 2 and table 1.

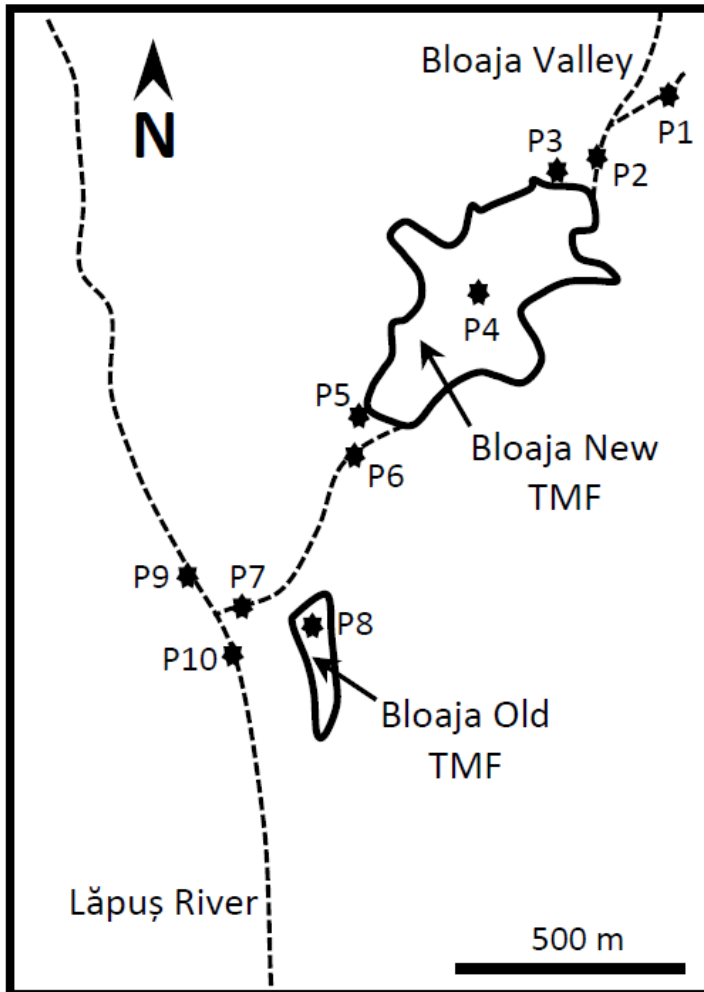


**Fig. 2.** Map of the sampling points from Bloaja Valley area

**Table 1.** *The site characteristics of water samples*

<b>Sample</b>	<b>Description</b>
P1	Small creek, left tributary of the Bloaja Valley, 200 m upstream of the Bloaja New TMF
P2	Surface water from the Bloaja Valley, 50 m upstream Bloaja New TMF
P3	Seepage water from the upstream dam of the Bloaja New TMF
P4	Surface water collected in the main channel of the diversion system constructed on the reclaimed pond
P5	Seepage water from the downstream dam of the Bloaja New TMF
P6	Surface water from the Bloaja Valley, 100 m downstream Bloaja New TMF
P7	Surface water from the Bloaja Valley, 50 m before the confluence with the Lăpuş River
P8	Surface water from the small pool located on the surface of the Bloaja Old TMF
P9	Surface water from the Lăpuş River, 100 m upstream to the confluence with the Bloaja Valley
P10	Surface water from the Lăpuş River, 100 m downstream to the confluence with the Bloaja Valley

The P1 and P2 samples were collected from pristine streams unaffected by the mining or other human activities and can be considered as reflecting the geochemical background of the study area. In order to assess the chemistry characteristics of the water due to the water-tailings interaction, three samples were analysed: P3, P5 are the seepages from the dams and P4 represents water drained from the surface of Bloaja New TMF in diversion channel. The P6 water was sampled from Bloaja Valley downstream Bloaja New TMF, considering that this sample reflects the impact of the flotation wastes on surface water. Located at 500 m downstream of the previous sample, the P7 comprise surface water from Bloaja Valley prior to the confluence with Lăpuş River. The sample water P8 was collected from a small pool formed by the accumulation on the surface of Bloaja Old TMF of meteoric water which interacted with the pyrite concentrate along the slope of the piles. Two samples of surface water (P9 and P10) from Lăpuş River were collected in order to evaluate the possible influence of Bloaja Valley tributary on the chemistry of river water.

Given the characteristics of the samples and their location, P1, P2, P6, P7, P9, and P10 can be considered as surface water samples. P3, P4, P5, and P8 are wastewater samples because the chemical characteristics of these waters resulted from the interaction with waste materials deposits: tailings facility and pyrite concentrate piles. To evaluate the quality of water samples, appropriate national regulations must be applied: Order 161/2006 for surface water and NTPA 001-2002 for wastewater.

In each sampling point, two subsamples were collected: one for pH, redox potential (Eh), electrical conductivity (EC), total dissolved solids (TDS) using a portable multiparameter (WTW Inolab 320i), the other was passed through a 0.2 µm filter and acidified with HNO<sub>3</sub> to pH < 2 for metal analysis. A ZEE nit 700 atomic absorption spectrometer using an acetylene–air flame, a graphite furnace and the adequate cathode lamps at the recommended current and conditions (specified in the FAAS Operators Manual) was used to determine the heavy metals content of four samples.

## RESULTS AND DISCUSSION

The values of physico-chemical parameters for the investigated water samples are presented in table 2.

**Table 2.** *The physico-chemical parameters of water samples*

Sample	pH	ORP (mv)	EC (µS/cm)	TDS (mg/l)
P1	6.26	16.9	165	82.5
P2	6.78	-2.8	265	132.5
P3	6.50	13.7	1997	998.5
P4	6.52	6.8	1039	519.5
P5	6.61	1.2	1782	891
P6	6.73	-3.2	481	240.5
P7	7.12	-26.8	470	235
P8	2.59	228.9	1564	782
P9	5.85	46.2	137	68.5
P10	6.31	21.3	171	85.5

All the samples except one show an acidic environment, the pH values ranging from 2.59 to 7.12 (figure 3). The slight acidic values are due to the geochemical background of the study area (P1, P2), the acid rock drainage caused by water-tailings interaction (P3, P4, P5, P6), and to the combination of the geochemical background and the mine wastes pollution (P9, P10). The lower value of pH (2.59 for P8) is the consequence of the intense acid rock drainage generated by the meteoric water which percolates the pyrite concentrate (a very rich sulphide material). A neutralization process is responsible for the neutral value of the pH for the P7 sample, the acidic water downstream Bloaja New TMF being diluted by small tributary creek of Bloaja Valley, unaffected by acid rock drainage.

Comparing P9 and P10 sampled from Lăpuş River (figure 4), it can be observed a slight increase of the pH, caused by the neutral water influx

of Bloaja Valley tributary. The mixing of acidic water from Lăpuș River with neutral water from Bloaja Valley has a limited neutralization effect due to the lower water flow of the valley compared to the river. The pH values measured in all samples fall within the limits (6.5 – 8.5) provided by national legislation (Order 161/2006, NTPA 001-2002).

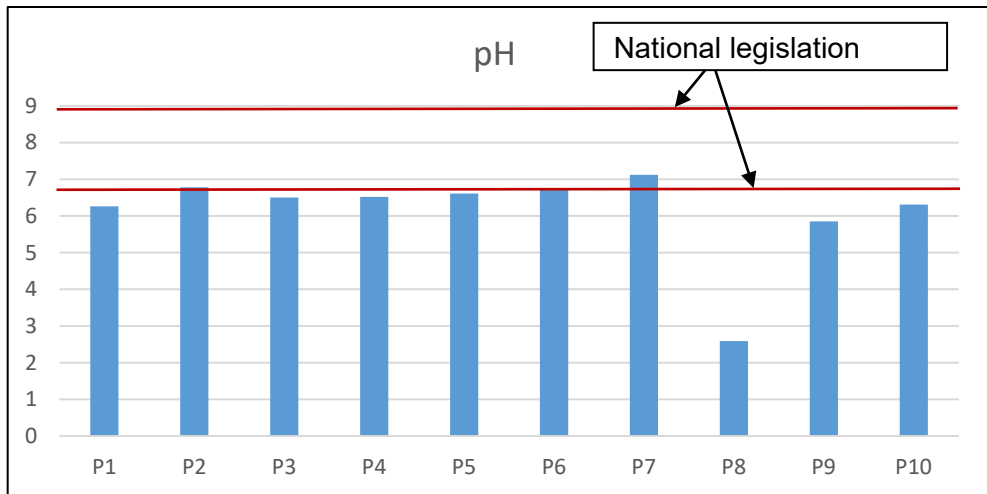


**Fig. 3.** The pH values of analyzed samples

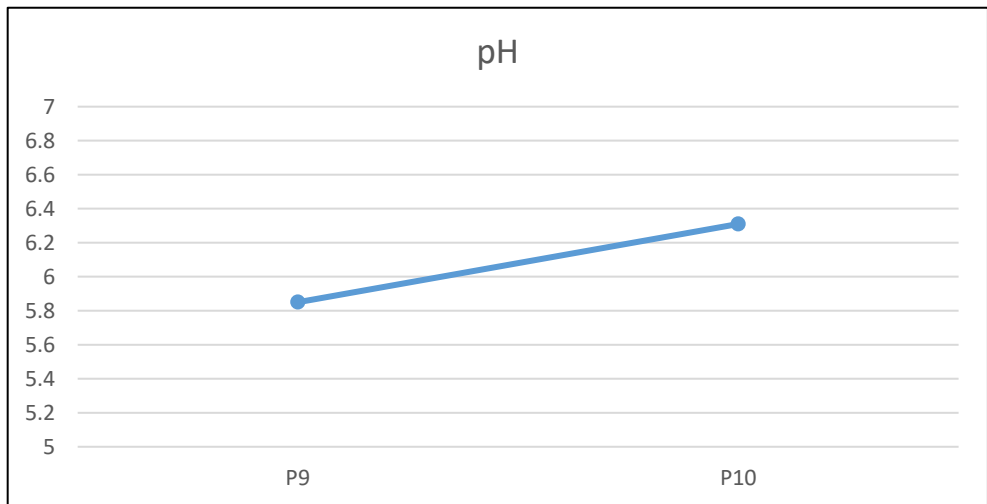


**Fig. 4.** The pH variation of Lăpuș River samples, upstream and downstream of Bloaja Valley confluence

CHEMICAL PARAMETERS OF BLOAJA VALLEY WATER AFFECTED BY ACID ROCK DRAINAGE,  
BĂIUȚ MINING AREA, ROMANIA

The TDS values ranges from small values (68.5 mg/l for P9) to higher values (998.5 mg/l for P3) (figure 5). Small TDS concentrations (below 150 mg/l) are specific to unpolluted water (P1, P2) or to the diluted water as a consequence of the high water flow of the River Lăpuș (P9, P10). The medium values of the TDS (P6, P7) are due to the starting of a neutralization process as a result of mixing with unpolluted waters.

Acid rock drainage influenced waters (P3, P4, P5, P8) show the higher concentration of TDS, above 500 mg/l. It can be noticed that the TDS values of the seepages from the upstream dam (P3) and the downstream dam (P5) are higher than the TDS value of the water sample collected form the diversion channel (P4). This difference of the acid rock drainage concentration is due to the longer interaction time between tailings and water necessary to generate seepages than specific for runoff waters. The higher value of the TDS for P3 and P5 (tailings dam's seepages) comparing to the TDS value of P8 (small pool from pyrite concentrate piles) can be explained by the longer time of the water-tailings interaction than the water-pyrite concentrates as a consequence of the material volume which is bigger in the case of tailings.

A slight increase of TDS value can be reported in the case of the two samples collected form Lăpuș River, upstream (P9) and downstream (P10) of the confluence to Bloaja Valley (figure 6). The TDS concentration of Bloaja Valley water (P7) is higher than that of Lăpuș River water upstream of the confluence.

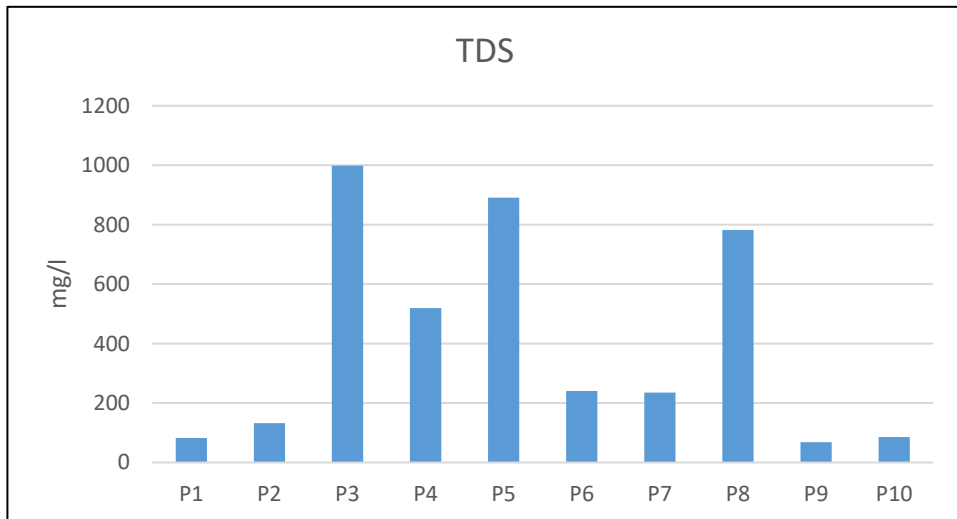


**Fig. 5.** The TDS values of analyzed samples

Due to the mineral characteristics of the tailings and pyrite concentrate, the Zn, Cu, Pb, Cd, and Ni contents in the waters that interacted with these wastes have been measured for P3, P4, P5, and P8. The metal concentrations of the seepages from the dams (P3, P5) and the water collected from diversion channel (P4) are low (table 3).

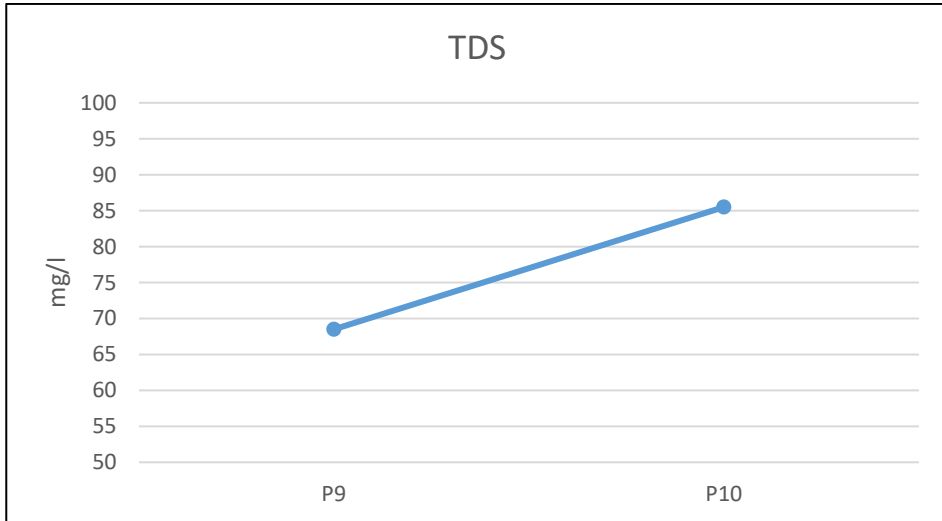


**Fig. 6.** The TDS variation of Lăpuș River samples, upstream and downstream of Bloaja Valley confluence

**Table 3.** Metal concentrations of the contact water samples with mining wastes

Sample	Zn (mg/l)	Cu (mg/l)	Pb (mg/l)	Cd (mg/l)	Ni (mg/l)
P3	0.129	ND	0.07668	ND	0.0440
P4	0.639	ND	0.03787	ND	0.0840
P5	0.197	ND	0.08614	ND	0.0212
P8	3.382	4.397	0.509	0.035	0.151
NTPA 001-2002	0.5	0.1	0.2	0.2	0.5

ND – non detected

The copper concentration for P4 is the only value which is higher than national standard NTPA 001-2002 and Government Decision 352/21.04.2005. Despite the fact that acid rock drainage is generated in the tailings, due to the small content of the sulphides in waste materials the metal concentration

is low. Conversely, in the case of water sample which interacted with the pyrite concentrate (P8) the metal concentration is very high, especially for Zn, Cu, and Pb.

Reporting these values to the relevant national legislation (NTPA 001-2002, Government Decision 352/21.04.2005), the Zn concentration is six times higher, the Cu concentration is forty-three times higher and the Pb concentration is two times higher than maximum allowable limits (figure 7). These values can be explained by the mineral composition of the pyrite concentrate. During the pyrite flotation process, small quantities of other metal sulphide are separated in addition to iron sulphide. Accordingly, the metal concentrations of acid rock drainage generated by the water percolation of the pyrite concentrate piles are higher than the contact water collected from the TMF.

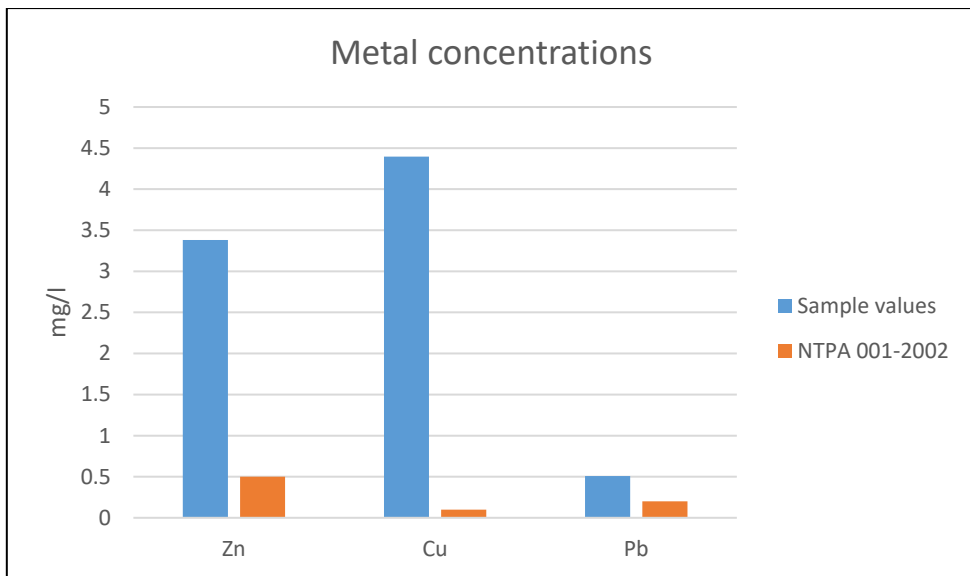


**Fig. 7.** Zinc, copper, and lead concentrations of P8 water sample compared with maximum allowable limits from national legislation

## CONCLUSION

The historical mining activity in the Băiuț area has led to the accumulation of some environmental problems whose consequences are still present today. After the mine closure, some rehabilitation works were done in order to reduce the environmental impact of mine facilities (underground

mine and tailings management facilities). However, these post-closure operations did not have a significant effect on acid rock drainage generated in underground mine works and mine wastes, Băiuț area being a surface waters pollution hotspot for Someș Basin. Such a source of pollution are the two tailings management facilities located on Bloaja Valley. The water which percolates the mining residues has a low pH and increased TDS values. Very high metal concentrations (Zn, Cu, Pb) were recorded for the contact water with the pyrite concentrate. All the acid rock drainage affected waters are discharged in Bloaja Valley, a left tributary of Lăpuș River. Due to the higher flow of the Lăpuș River than that of the Bloaja Valley, the effect of the discharged waters from TMFs is not very conspicuous.

Further studies are necessary in order to determine the chemistry of water unaffected by human (especially mining) activities that is closely related to geochemical background. A new more complex rehabilitation program would reduce the environmental risk associated with acid rock drainage and its impact on the surface water.

## REFERENCES

- Achim V., Ciolte A., 1991, Băiuț. Technical and monographic documentary. *Gutinul Publishing House*, Baia Mare, 306 p [in Romanian].
- Aroldi C., 2001, *The Pienides in Maramureș: sedimentation, tectonics and paleogeography*. Ed. Presa Universitară Clujeană, 156 p.
- Bird G., Brewer P.A., Macklin M.G., Bălțeanu D., Driga B., Șerban M., Zaharia S., 2003, The solid state partitioning of contaminant metals and As in river channel sediments of the mining affected Tisa drainage basin, northwestern Romania and eastern Hungary. *Applied Geochemistry*, **18**, pp. 1583-1595.
- Borcoș M., Gheorghită I., 1976, Neogene hydrothermal ore deposits in the volcanic Gutâi Mountains. IV. Băiuț – Văratec – Botiza metallogenic field. *Rev. Roum. Geol., Geophys. et Geogr., Geologie*, **20** (2), pp. 197-209.
- Candeias C., Avila P., Coelho P., Teixeira J.P., 2018, Mining activities: health impacts. *Encyclopedia of Environmental Health*, 2nd Edition, <https://doi.org/10.1016/B978-0-12-409548-9.11056-5>.
- Chira I., Damian G., Chira R., 2014, Spatial distribution of heavy metals in the soils of Băiuț area, Maramureș County, Romania. *Carpathian Journal of Earth and Environmental Sciences*, **9** (1), pp. 269 – 278.
- Costin D., 2000, Major elements geochemistry of the Breiner Băiuț ore deposit (Gutâi Mts., Eastern Carpathians). *Studia Universitatis Babeș – Bolyai, Geologia*, **XLV** (1), pp. 55-66.

- Costin D., 2007, Genetic factors and environmental impact of acid mine drainage at Văratec Băiuț mine, Baia Mare district, Romania. *Studia Universitatis Babeș-Bolyai, Ambientum*, **1** (1-2), pp. 75-85.
- Costin D., Baciuc C., 2010, Environmental risks associated to acid mine drainage in Baia Mare mining region, Romania. *Central European Journal of Occupational and Environmental Medicine*, **16** (1-2), pp. 19-30.
- Costin D., Marina B., 2006, Environmental impact of Văratec Mine, Băiuț region (Maramureș) on surface waters. *Romanian Journal of Mineral Deposits*, **82**, pp. 61-65.
- Costin D., Vlad Ș., 2005, Ore formation at Văratec – Băiuț, Baia Mare region, East Carpathians, Romania. *Geochemistry, Mineralogy and Petrology*, **43**, pp 64-68.
- Doroșan D., Costin D., Ozunu A., 2018, Application of quality indices for evaluation of heavy metals pollution in water, soil and sediments in the upper Lapuș river, Băiuț mining district, Maramureș county, Romania. *Journal of Environmental Protection and Ecology*, **19** (4), pp. 1472-1480.
- Doroșan D., Ozunu A., Costin D., 2015, Accumulation of heavy metals in soils and alluvial deposits of Lăpuș River, Maramureș County, Romania. *Carpathian Journal of Earth and Environmental Sciences*, **10** (4), pp. 181-190.
- Government Decision 352/21.04.2005 on the modification and completion of the Government Decision no. 188/2002 approving some norms regarding the discharge conditions in the aquatic environment of the waste waters, Romanian Official Monitor No. 398/11.05.2005 [in Romanian].
- Kossoff D., Dubbin W.E., Alfredsson M., Edwards S.J., Macklin M.G., Hudson-Edwards K.A., 2014. Mine tailings dams: characteristics, failure, environmental impacts, and remediation. *Applied Geochemistry*, **51**, pp. 229-245.
- Maramureș County Committee for Emergency Situations, 2016. Analysis plan and risk coverage for Maramureș County, 126 p.
- Matschullat J., Ottenstein R., Reimann C., 2000, Geochemical background – can we calculate it? *Environmental Geology*, **39** (9), pp. 990-1000.
- Nordstrom D.K., 2011. Mine waters: acidic to circumneutral. *Elements*, **7**, pp. 93–98.
- NTPA 001-2002 regarding the establishment of pollutant loading limits for industrial and urban wastewater for discharge into natural receptors, Romanian Official Monitor, No. 187/20.03.2002 [in Romanian].
- Order 161/2006 approving the Normative for classification of surface water quality to set the ecological status of water bodies, Romanian Official Monitor No. 511/13.06.2006 [in Romanian].
- Skousen J.G., Ziemkiewicz P.F., McDonald L.M., 2019, Acid mine drainage formation, control and treatment: approaches and strategies. *The Extractive Industries and Society*, **6**, pp. 241–249.



## PLATINUM RECOVERY FROM USED AUTO CATALYSTS: DISSOLUTION AND PRECIPITATION STUDIES

Angela M. KASZA<sup>1</sup>, Gabriel KATONA<sup>2,3</sup>, Monica DAN<sup>1</sup>, Cezara VOICA<sup>1</sup>,  
Oana GRAD<sup>1</sup>, Maria MIHEȚ<sup>1</sup>, Tibor DEZSO<sup>2</sup>, Ruben NAGY<sup>2</sup>, Tihamer BOTS<sup>2</sup>,  
Mihaela Diana LAZĂR<sup>1\*</sup>

<sup>1</sup>National Institute for Research & Development of Isotopic and Molecular Technologies –  
INCDTIM, 67–103 Donat Str., 400293 Cluj–Napoca, Romania

<sup>2</sup> SC Union Co SRL, Str. Tăietura Turcului 47, Parc Tetarom I, Cluj-Napoca, Romania

<sup>3</sup>Babes-Bolyai University, Faculty of Chemistry and Chemical Engineering,

11 Arany Janos Street, 400028 Cluj-Napoca, Romania

\*Corresponding author: [diana.lazar@itim-cj.ro](mailto:diana.lazar@itim-cj.ro)

**ABSTRACT.** Noble metals are used in a plethora of applications, from electronic and communication equipments, to aerospace engines, mobile phones and catalytic converters. Currently, there is a continuous interest in the recovery of noble metals from waste, as their natural reserves are limited. Herein, the paper presents studies on the recovery of platinum from spent automotive catalysts. The process involves two steps - dissolving of platinum, followed by its precipitation into a hexachloroplatinum complex. The optimum reaction conditions for dissolving Pt from the spent automotive catalyst use a mixture of H<sub>2</sub>O<sub>2</sub> + HCl (1:5.5 molar ratio) at 30°C, for 8 h. For the full recovery of platinum from the solution, the volumetric ratio of 4:1 between the platinum solution and the precipitating ammonium chloride solution is optimum. In addition, studies regarding the precipitation time and temperature have also been performed. All the obtained precipitates were analyzed by X-ray powder diffraction and showed the structure of the hexachloroplatinic (NH<sub>4</sub>)<sub>2</sub>[PtCl<sub>6</sub>] complex, with high purity. Upscaling of the processes for technological transfer show promising results in the recovery of platinum from spent automotive catalysts.

**Key words.** *Spent automotive catalyst, Pt recovery, (HCl + H<sub>2</sub>O<sub>2</sub>) leaching, precipitation.*

### INTRODUCTION

Protecting the environment against the polluting emissions of internal combustion engines, especially diesel ones, led the automotive industry to create catalytic systems containing metals from the platinum group. Catalytic

converters are part of the exhaust system in modern vehicles that help to reduce the dangerous gases produced by cars, such as CO, unburned hydrocarbons, and NO<sub>x</sub> (Venkateswarlu et al., 2019) The continuous increase in emission standards has led manufacturing companies to improve their automotive catalytic converter to comply with government regulations. The introduction of catalytic converters on the car market in 1975 generates an enormous amount of waste every year, consisting in used, inactive catalysts contained in spent converters. Also, the very high growth of the automobile industry in the last decade has led to a further increase in this waste (Kovalcik et al., 2021).

To carry out the reduction reactions, automotive catalytic converters mainly use platinum, palladium and rhodium known as platinum group metals (PGM). Spent catalysts are one of the most important secondary resources of PGMs. It is estimated that spent automotive catalytic converters deliver more than 57% of PGMs' European supply, being considered a crucial resource for PGM recovery (Yakoumis et al., 2021). In 2020, the automotive catalyst industry uses about 32% of total Pt, 85% of total Pd, and 90% of total Rh. The quantity of platinum, palladium and rhodium in auto catalysts depends mainly on the vehicle type, manufacturer, country, production year or other additional factors. In two ways converters platinum is the main catalytic metal, the ratio of Pt/Rh being 5 to 1, and the ratio of Pd/Rh 7 to 1, with actual concentration of platinum in a large range (from tens to thousands of ppm depending on the above-mentioned factors) (Fornalczyk et al., 2009).

Recovering PGM from the spent automotive catalysts can be realized by two methods: the pyrometallurgical and hydrometallurgical methods. The pyrometallurgical methods use high temperature (over 1600°C) generated by plasma or by electric arc furnace to melt the PGMs (Peng et al., 2017; Dong et al., 2015; Devyatykh et al. 2018). The second type of methods (hydrometallurgy) are more eco-friendly and offer several advantages: lower process temperature, lower energy consumption, higher purification yield, process control and economically profitability (Saguru et al, 2018; Rzelewska-Piekut and Regel-Rosocka, 2018; Asadzadeh and Sajadi, 2018).

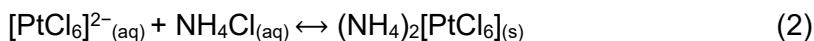
The hydrometallurgical processes are based on the dissolution of PGMs using strong oxidizing media, followed by the metal recovery from solution by selective precipitation and calcination. Among the three PGM metals, platinum is found in the largest quantities in used car catalytic converters and therefore is suitable for recovery by hydrometallurgical methods. Different leaching processes can be used for the dissolution of PGMs, all being combinations of hydrochloric acid and strong oxidizing agents (HNO<sub>3</sub>, Cl<sub>2</sub>, NaClO, NaClO<sub>3</sub>, H<sub>2</sub>O<sub>2</sub>, etc.) (Grumett, 2003; Marinho et al., 2011; Sun and Lee, 2011).

In this study, spent catalysts from unknown producers were used to develop a more eco-friendly and low energy consuming method for platinum recovery than the usual patented methods. For the solubilization of the platinum from waste catalysts, HCl and H<sub>2</sub>O<sub>2</sub> as oxidizing agents are used, avoiding thus the usage of nitric and sulfuric acids, which generate harmful gaseous and liquid wastes. The reduction potential of the H<sub>2</sub>O<sub>2</sub> shows that it is capable to solubilize platinum, providing favorable reaction kinetics (Barakat et al., 2006). The reaction of dissolution undergone by platinum is described by the following equation:



where subscript aq and s represent aqueous and solid, respectively.

This step is followed by filtration and selective reduction of the formed platinum complexes (PtCl<sub>6</sub><sup>2-</sup>) by NH<sub>4</sub>Cl (Burkin, 2001).



The reaction needs saturated ammonium chloride solution which was added to the hexachloroplatinic acid solution in order to precipitate diammonium hexachloroplatinate complex (Barakat and Mahmoud, 2004)

## EXPERIMENTAL

### Materials and Chemicals

Spent automotive catalysts with a honeycomb structure were ground and sieved to a particle size fraction lower than 1 mm. Chemicals used for the leaching procedure were hydrochloric acid (HCl, 37%) and hydrogen peroxide (H<sub>2</sub>O<sub>2</sub>, 30%, w/w) solutions from Honeywell-Fluka, used as purchased. Ammonium chloride (NH<sub>4</sub>Cl) employed for the precipitation procedure was used as received from VWR Chemicals. Double distilled water was used throughout the experimental procedures.

### Instruments

Inductively coupled plasma quadrupole mass spectrometry (ICP-MS, ELAN DRC-e, Perkin Elmer) was used for elemental analysis and concentration measurements. X-ray powder diffraction (XRD) measurements were made using a Bruker D8 Advanced Diffractometer with Cu Kα1 radiation, 40 kV operating voltage and 40 mA current.

## RESULTS AND DISCUSSIONS

### Leaching of Platinum from the spent automotive catalysts

The choice of leaching procedure of platinum from spent automotive catalysts was motivated, besides the Pt recovery efficiency, by safety and environmental reasons if employed in a dedicated facility, and not in a specialized laboratory. Thus, although several Pt leaching procedures proved their efficiency, for the purpose of this work, a mixture of  $H_2O_2$  and HCl in a molar ratio of 1:5.5 was used. By means of this mixture, leaching of Pt from the spent automotive catalysts undergoes as described in Introduction.

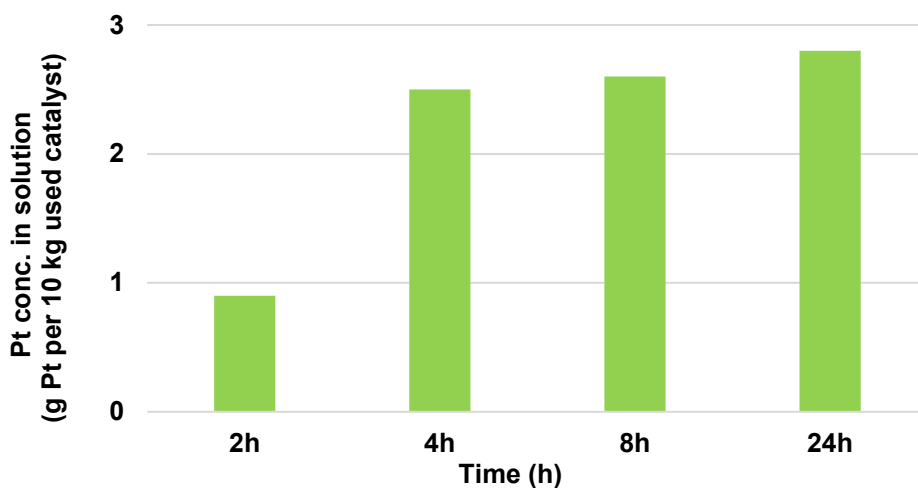


**Fig. 1.** The influence of dissolving time on the Pt concentration in the leached solution (conditions: 0.5 g used catalyst; 0.68 ml  $H_2O_2$  (conc) + 3.13 ml HCl (conc); molar ratio = 1: 5.5, 30°C).

In order to optimize the leaching procedure by means of  $H_2O_2+HCl$ , the influence of dissolving time was evaluated. Thus, several reaction mixtures using the same amounts of grounded spent catalyst and  $H_2O_2$  and HCl solutions were stirred in round bottom flasks at 30°C for different time ranges. For a better understanding, the amount of Pt leached from the spent automotive catalyst was expressed as grams of Pt per 10 kg of catalyst. Figure 1 illustrates the variation of dissolved Pt from the spent catalyst as a function

of time. It may be observed that the longer the reaction time, the greater the amount of Pt recovered from the spent catalyst. However, the amount of dissolved Pt from the solid catalyst increases to a very low extent if the reaction time increases from 4 to 24 h. It may be concluded that the optimum reaction time for dissolving Pt from the spent automotive catalyst with a mixture of  $\text{H}_2\text{O}_2 + \text{HCl}$  (1:5.5 molar ratio) at  $30^\circ\text{C}$  is 8 h.

### **Precipitation of Platinum from the leached solutions**

Platinum can be separated from the acidic leached solution by precipitation with ammonium chloride, as described in Introduction. In this precipitation reaction, the molar ratio of the reactants and temperature are among the most important variables. These parameters can be varied in a wide range, from 1:5 to 1:40 (Nguyen et al., 2022) and  $25\text{-}80^\circ\text{C}$  (Nagai et al., 2017), respectively, and the outcome of the precipitation reaction depends on the initial platinum content of the solution. It should be accounted that the solubility of the hexachloroplatinic complex is rather high, therefore finding the right conditions to precipitate the Pt complex without its further dissolving, in order to maximize the recovered amount of Pt, is of utmost importance.

Thus, optimization of the precipitation procedure was pursued by investigating the influence of several parameters such as: (a) volume of saturated  $\text{NH}_4\text{Cl}$  solution; (b) temperature; (c) reaction time. Upscaling of the precipitation procedure was also pursued by investigating the amount of platinum solution which can be efficiently treated. Each precipitation experiment was performed using an initial leached acidic Pt solution with a concentration of 155 mg Pt/L and a saturated solution of  $\text{NH}_4\text{Cl}$  (45 g  $\text{NH}_4\text{Cl}$  to 100 mL  $\text{H}_2\text{O}$ , dissolved at  $40^\circ\text{C}$ ).

#### ***(a) Influence of saturated $\text{NH}_4\text{Cl}$ solution volume***

The addition of supplementary  $\text{NH}_4\text{Cl}$  precipitating agent is accompanied by the presence of extra water in the system, which highly affects the precipitation – dissolution process due to the very low concentration of Pt in the initial leaching solution (figure 2). It was established that, for the platinum solution used in this study, the volumetric ratio of 4:1 between the platinum solution and the precipitating solution is optimum. The rest of the parameters were optimized using this ratio between the reagents.

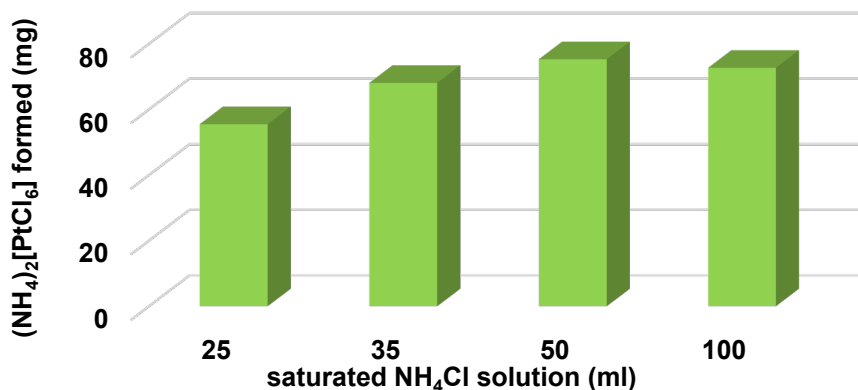


**Fig. 2.** The influence of  $\text{NH}_4\text{Cl}$  quantity on the formation of the platinum precipitate (conditions: 200 ml platinum solution; 15 minutes reaction time;  $40^\circ\text{C}$ ).

### (b) Influence of temperature

Three temperature values were tested for the precipitation of 200 ml leached Pt solution with the determined optimum volume of saturated  $\text{NH}_4\text{Cl}$  solution of 50 ml. As illustrated by the results presented in figure 3, it may be observed that the amount of formed platinum precipitate increases to a very low extent with increasing reaction temperature. If at  $40^\circ\text{C}$  73 mg of  $(\text{NH}_4)_2[\text{PtCl}_6]$  is formed, by doubling the temperature only a benefit of 3 mg of precipitate is obtained (an enhancement of 5.5 %), which does not economically justify the extra amount of employed energy. Thus, it may be concluded that the optimum precipitation temperature is  $40^\circ\text{C}$ .

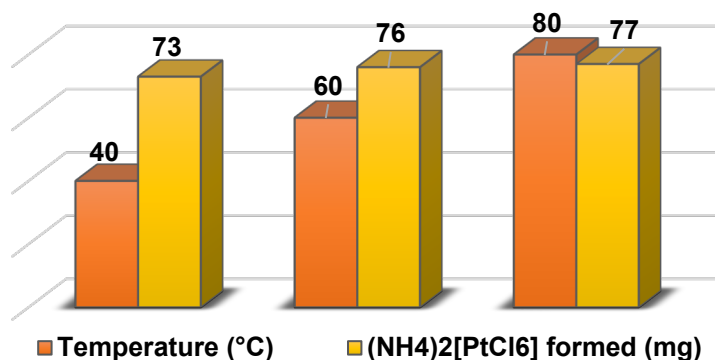


**Fig. 3.** The influence of temperature on the formation of the platinum precipitate (conditions: 200 ml platinum solution; 50 ml saturated  $\text{NH}_4\text{Cl}$  solution; 15 minutes reaction time).

### (c) Influence of reaction time

Considering the rather high solubility of the Pt complex, this should be removed from the solution in order to avoid its further dissolving. However, the precipitate does not form immediately after the saturated  $\text{NH}_4\text{Cl}$  solution is added to the leached Pt solution, but slowly starts to form under the stirring conditions. Therefore, in order to find the optimum reaction time for the formation of the platinum precipitate, six precipitation experiments were performed using 200 ml Pt solution and 50 ml saturated  $\text{NH}_4\text{Cl}$  solution at  $40^\circ\text{C}$ , in the time range 5 – 120 min. Results presented in figure 4 show that the highest amount of  $(\text{NH}_4)_2[\text{PtCl}_6]$  precipitate is obtained after only 5 min of reaction, while any other increase in the reaction time leads to a decrease in the obtained amount of precipitate as a consequence of its partial dissolving in the solution. It can be observed that after 15 minutes, the equilibrium between precipitation and dissolution is reached. It may be concluded that a 5 min reaction time is the necessary required time to precipitate the largest amount of  $(\text{NH}_4)_2[\text{PtCl}_6]$ . This reaction time was further used for the upscaling experiments.

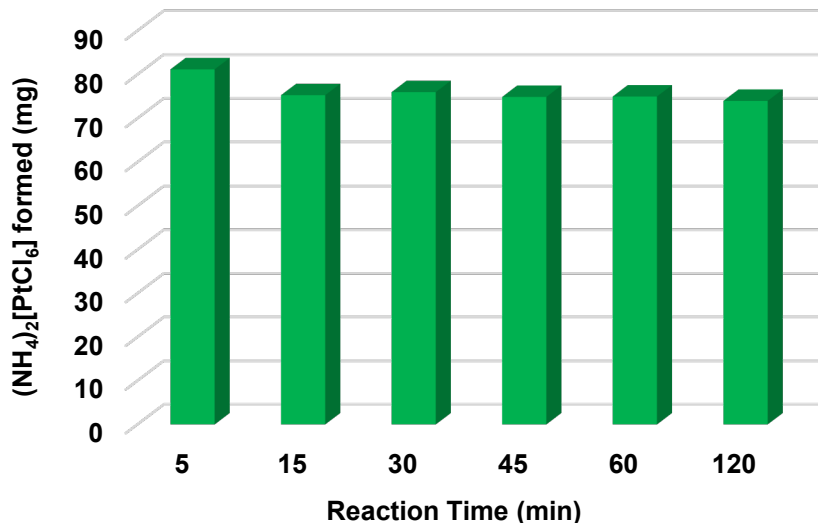


**Fig. 4.** The influence of reaction time on the formation of the platinum precipitate (conditions: 200 ml platinum solution; 50 ml saturated  $\text{NH}_4\text{Cl}$  solution;  $40^\circ\text{C}$ ).

### ***(d) Structural analysis of $(\text{NH}_4)_2[\text{PtCl}_6]$ complex and precipitation degree analysis***

In order to confirm the formation of the hexachloroplatinic complex, and also to check its purity, the obtained precipitates were analyzed by powder X-ray diffraction (XRD). The measured diffractograms were identical for all the above experiments and proved the reproducibility of the precipitation and separation of  $(\text{NH}_4)_2[\text{PtCl}_6]$ . The comparison of the experimental pattern with the one from XRD database proved the identity of ammonium hexachloroplatinate complex (figure 5). No other additional diffraction peaks were identified.

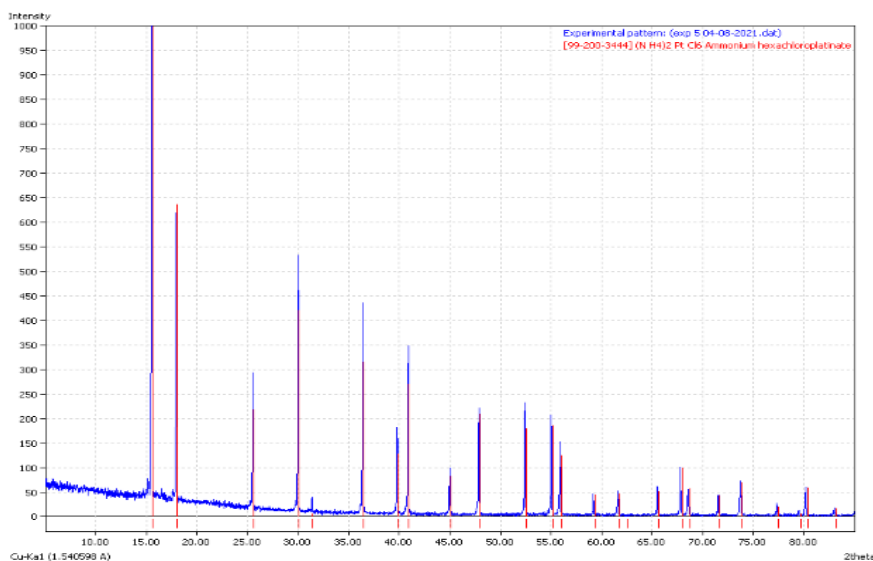


**Fig. 5.** XRD pattern of the platinum precipitate.

The balance of the platinum element has been calculated. The initial solution (200 ml) contains 32 mg of platinum while the precipitate (81 mg) incorporates 33 mg of platinum element. This is indicative for a total recovery of platinum from the solution, by using the optimized reaction conditions.

### ***(e) Upscaling of the precipitation procedure***

Scale up batches were performed in order to demonstrate the feasibility of the precipitation process to be later transferred to a pilot technology. The volume of initial solution has been doubled step-by-step up to 800 ml, while the quantity of the formed precipitate increased linearly, with

the same increment (figure 6). The quality of the platinum precipitate was measured for each experiment. The results showed that high purity ammonium hexachloroplatinate was formed every time. This shows the real potential of this process to be transferred into production.

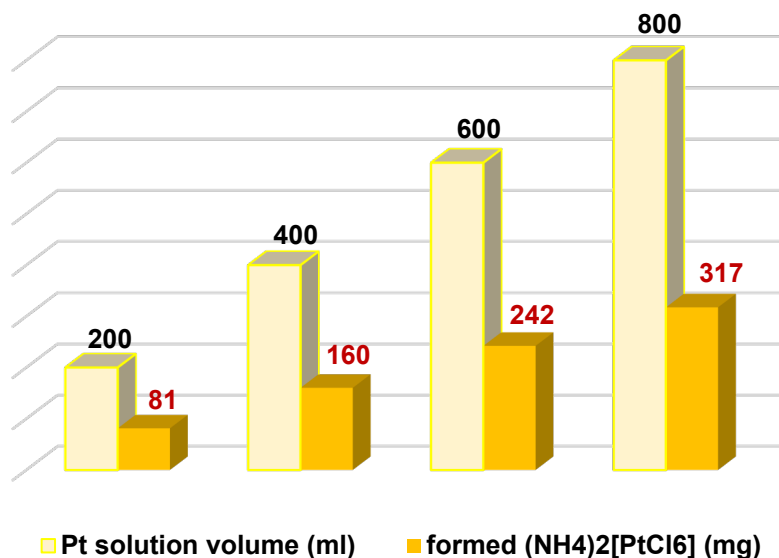


**Fig. 6.** Upscaling of the platinum precipitation process; (conditions: 40°C; 5 minutes reaction time).

## CONCLUSIONS

An optimized method for platinum recovery from real spent auto catalysts was developed. The method comprises two steps: platinum dissolution from catalysts and platinum recovery from acid leaching solutions as ammonium hexachloroplatinate. The optimum parameters of recovery method are: (i) dissolution in  $\text{HCl} + \text{H}_2\text{O}_2$  solution (molar ratio = 1 : 5.5), at 30°C for 8h; (ii) the volumetric ratio of leached platinum solution and the saturated  $\text{NH}_4\text{Cl}$  solution is 4:1; (iii) precipitation temperature 40°C; (iv) precipitation time 5 minutes.

High purity ammonium hexachloroplatinate is obtained from platinum acid solution using the optimised parameters.

The precipitation method was scaled up to 800 mL platinum solution proving its potential to be further transferred and adapted for higher scale (pilot scale).

### Acknowledgement

This work was supported by a grant of the Romanian Ministry of Education and Research, CCCDI – UEFISCDI, project number PN-III-P2-2.1-PTE-2019-0606, within PNCDI III. The authors thank dr. Alexandru Turza for XRD measurements.

### REFERENCES

- Asadzadeh M., Sajadi S.A.A, 2018, Separation and Recovery of Platinum and Palladium from Spent Petrochemical Catalysts Using Activated Carbon, Analysis of Two Kind of Most Used Catalysts in Petro Chemistry. *Iran. J. Chem. Chem. Eng.*, **37**, pp. 9-18.
- Barakat M.A., Mahmoud M.H.H., 2004, Recovery of platinum from spent catalyst. *Hydrometallurgy*, **72**, pp. 179-184.
- Barakat M.A., Mahmoud M.H.H., Mahrous Y.S., 2006, Recovery and separation of palladium from spent catalyst. *Appl. Catal. A: General*, **301**, pp. 182-186.
- Burkin A.R., 2001, Chemical Hydrometallurgy: Theory and Principles, Imperial College Press, London.
- Devyatykh E. A., Devyatykh T. O., Boyarsky A. N., 2018, Overview of technologies for extraction of platinum group metals from poor raw materials. *KnE Engineering*, pp. 154-160.
- Dong H., Zhao J., Chen J., Wu Y., Li B., 2015, Recovery of platinum group metals from spent catalysts: a review. *Int. J. Miner. Process.*, **145**, pp.108-113.
- Fornalczyk A., Saternus M., 2009, Removal of platinum group metals from the used auto catalytic converter. *Metalurgija*, **48**, pp. 133-136.
- Grumett P., 2003, Precious metal recovery from spent catalysts. *Platin. Met. Rev.*, **47** (4), pp. 162–166.
- Kovalcik J., Straka M., Kacmary P., Pavlik T., 2021, Catalyst Processing and Recycling. *Acta Technol.*, **7** (3), pp. 99-104.
- Marinho R.S., da Silva C.N., Afonso J.C., da Cunha J.W., 2011, Recovery of platinum, tin and indium from spent catalysts in chloride medium using strong basic anion exchange resins. *J. Hazard. Mater.* **192** (3), pp. 1155–1160.
- Nagai H., Shibata E., Nakamura T., 2017, Recovery of Ruthenium from a Solution Containing Platinum Group Metals. *J. Jpn. I. Met.*, **81** (4), pp. 178-185.
- Nguyen V.N.H., Song S.J., Lee M.S., 2022, Selective precipitation of ammonium hexachloropalladate from leaching solutions of cemented palladium with zinc. *Journal of Mining and Metallurgy, Section B: Metallurgy*, <https://doi.org/10.2298/JMMB220208013N>.

- Peng Z., Li Z., Lin X., Tang H., Ye L., Ma Y., Rao M., Zhang Y., Li G., Jiang T., 2017, Pyrometallurgical Recovery of Platinum Group Metals from Spent Catalysts. *JOM: the journal of the Minerals, Metals & Materials Society*, **69** (9), pp. 1553-1562.
- Rzelewska-Piekut M., Regel-Rosocka M., 2018, Wastes generated by automotive industry- spent automotive catalysts. *Phys. Sci. Rev.*, **3** (8), pp. 20180021.
- Saguru C., Ndlovu S., Moropeng D., 2018, A review of recent studies into hydrometallurgical methods for recovering PGMs from used catalytic converters. *Hydrometallurgy*, **182**, pp. 44-56.
- Sun P.P., Lee M.S., 2011, Separation of Pt from hydrochloric acid leaching solution of spent catalysts by solvent extraction and ion exchange. *Hydrometallurgy*, **110** (1-4), pp. 91–98.
- Venkateswarlu K., Kumar R.A., Krishna R., Sreenivasan M., 2019, Modeling and fabrication of catalytic converter for emission reduction. *Mater. Today: Proc.*, **33**, pp. 1093-1099.
- Yakoumis I., Panou M., Moschovi A.M., Pantias D., 2021, Recovery of platinum group metals from spent automotive catalysts: A review. *Cleaner Eng. Technol.*, **3**, 100112.



## POLYURETHANE WASTE UTILIZATION

Dorin Iosif MANCIULA<sup>1\*</sup>, Radu Barbu Horațiu MIȘCA<sup>2</sup>, Andrei ROTER<sup>1</sup>

<sup>1</sup>*Babeș-Bolyai University, Faculty of Environmental Science and Engineering,  
30 Fântânele Street, Cluj-Napoca, Romania*

<sup>2</sup>*Babeș-Bolyai University, Faculty of Chemistry and Chemical Engineering,  
11 Arany János Street, Cluj-Napoca, Romania*

*\*Corresponding author: iosif.manciula@ubbcluj.ro*

**ABSTRACT.** Following the explosive development of industrial processes in recent decades, society began to feel more and more the need for efficient measures to prevent pollution on a global scale, or finding new, or alternative resources. Such a measure is to reuse as much material as possible, that we now consider waste or residue, to reduce the consumption of resources, especially non-renewable resources. In this regard, the paper presents a way to recycle polyurethane waste and obtaining a composite material by mixing it with a fresh polyurethane adhesive and quartz sand in different proportions. The polyurethane wastes thus become a substitute for pure polyurethane, and the obtained mixture may be used for manufacturing construction materials. The samples were studied in terms of physical properties and behavior under the action of some environmental factors.

**Key words:** *waste and polyurethane foams, polymeric composite materials, construction materials, insulation materials.*

### INTRODUCTION

Polyurethanes (PU) are synthetic polymers produced by the polyaddition reaction of a diisocyanate or a polymeric isocyanate with a diol or polyol, in the presence of catalysts and additives. A virtually unlimited number of chemical structures can be obtained under the name of PU, the only condition being the presence of urethane group within the macromolecular chain at certain intervals. Urethane group is formed, usually by the reaction between the isocyanate and the hydroxyl group, although it may be formed from phosgene and di- or polyamines in some special cases (Sharmin and Zafar, 2012).

Due to the multitude of possible chemical structures and arrangement of molecules in the chain structure, PU is a good example of polymer with guided structure in order to obtain a wide range of materials with channeled physico-chemical properties (controlled structures). The properties of polyurethanes (thermoplastic or thermoset) depend largely on their macromolecular structure, i.e., the nature and macro functionality monomers constituents (Xu et al., 2008). PU can be obtained in a wide range of variations of the physico-chemical properties. The main types of PU are rigid polyurethane, flexible polyurethane (elastic PU), thermoplastic polyurethane and porous polyurethane (Kapps and Bushkamp, 2004).

This material is extremely versatile in structure and properties, combines the elasticity of rubber with the durability and strength of metals, which allows its use as a substitute for the long-term replacement of materials such as plastic, rubber or some metals, required in highly stressed environments. Due to the unique properties they possess such as tensile strength, tear, compression, high hardness, high elongation at break and a high elasticity modulus, polyurethanes are employed mainly as construction materials, thermal and acoustic insulation, for filling inoperative gaps, as adhesives, in textile industry, as material for packaging of sensitive and high-priced products, in footwear industry, in mining and ore processing, transport, paper and pulp processing, energy and sports equipment, (Goods et al., 1997; Kojio et al., 2010; Mounanga et al., 2008).

PU world consumption is steadily increasing due to their various use and advantageous economic properties, (Priscariu, 2011). Uses of PU is also reflected on their main components, especially isocyanates, polyols, auxiliary substances, catalysts, or substances used in producing rigid foams, fibers, paints and varnishes, elastomers, automotive applications in car body repair and as insulating building materials. Polyurethane "spray-on" type of products containing isocyanate, are used as protective coating for concrete, wood, fiberglass, steel and aluminum (Böer et al., 2014).

The increasing use of polyurethane products resulted in increased quantities of PU waste, which must be processed. Currently, there are three methods available for waste processing, respectively incineration, disposal to landfill and recycling or reuse. Of these, recycling and reusing materials offers the best solution in terms of the impact on the environment and human health, since there is no waste that cannot be salvaged or toxic gases after processing them. The most effective methods of recycling and destruction, both physical and chemical, must ensure not only compliance with safety and environmental pollution prevention, but also lowering the production costs of materials obtained from recycled PU (Howarth, 2003; Yang et al., 2012; Zevenhoven, 2004).

## EXPERIMENTAL PART

The experimentation aimed to achieve a method in which polyurethane wastes are reprocessed by mixing them with fresh polyurethane adhesive and quartz sand, thus generating a new composite material that can be used as a substitute for pure polyurethane in the building materials industry. The method used for recycling the polyurethane waste involves, in a first phase, the modification of the size and shape of the material. Experimentally it has been observed that crushing and shredding wastes are effective methods to recycle and reuse thermosetting materials.

For the next step, the working procedure consisted of physico-mechanical treatment of crushed PU wastes, by using a filling material, such as a polyurethane adhesive for binding the particles to each other, under continuous stirring to obtain the samples. The work stages are presented in the operating scheme (figure 1).

During experiments were used the following materials and equipment: polyurethane foam, polyurethane adhesive, quartz sand fraction 0.1 - 0.62 mm, plastic molds (petri dish), mold release agent, mixer with rotating blades, analytical balance and a heating oven.

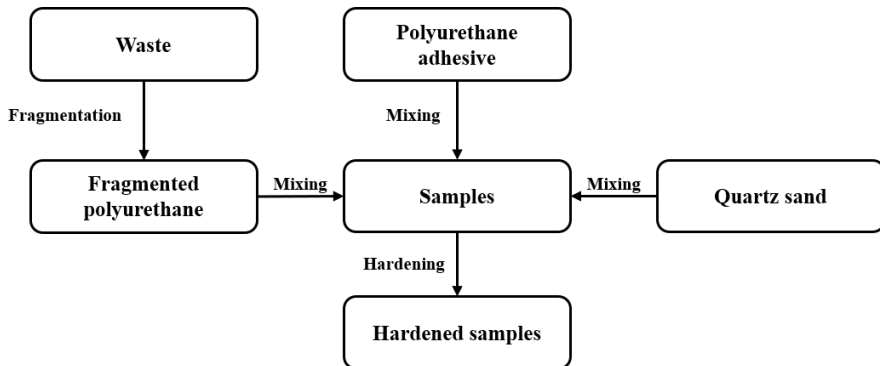


**Fig. 1.** *The operating scheme.*

The polyurethane waste (figure 2a) was fragmented with the aid of a cutting type mixer with rotating blades and speed control (figure 2b), after which it was mixed with a polyurethane adhesive (samples 1 - 5) and quartz sand (samples 6 - 10) in different proportions. The mixture was then poured into molds and held 4 days to cure at 32 - 35 °C, after which they were removed from the molds (figure 2 c - d).

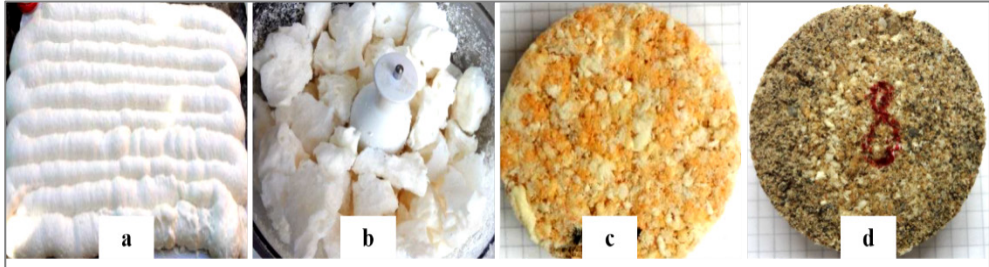


**Fig. 2.** *a. Waste from polyurethane foam. b. Material fragmentation. c. The hardened sample from the mixture of PU waste and PU adhesive. d. The hardened sample from the mixture of PU waste, PU adhesive and sand.*

To obtain the optimum mix of adhesive and fragmented polyurethane material, attempts were made to obtain a homogeneous mixture in a short time. The experiments have been carried out in three different modes by using the same amounts of material. In first method, the crushed material was added onto the adhesive and then the mixture has been stirred continuously, then during the second method, over the shredded material, the adhesive was poured out under continuous stirring, and last, the shredded material and the adhesive were simultaneously added while constantly mixing them together. The last method has provided the best results to get in a short time a homogenous material on a macroscopic scale.

For each sample, the apparent density was determined. All samples were immersed next in water and maintained immersed for 7 - 14 days to determine the liquid retention inside the material.

## RESULTS AND DISCUSSIONS

The recycling method is simple and easy to implement, and the costs are relatively low. The best results regarding the hardening of the adhesive and the quality of the final material were obtained at a temperature between 32 - 35 °C for 4 days, (table 1). Before pouring the mixture into the molds, they were covered with the release agent to prevent the samples from sticking to them.

Samples 1 - 5 were prepared by making homogenous mixture of PU waste material and freshly PU adhesive in different proportions (table 1). The samples were left to harden in plastic molds inside the oven at 32 °C for 4 days. It has been observed that the polyurethane material was cured

completely into the mold. Samples 6 - 10 were prepared by mixing the crushed PU waste material in plastic molds with fresh PU adhesive and sand in varying proportions (table 1) to obtain a homogenous mixture. All samples were kept in the oven to harden at 35 °C for 4 days. Adding sand to the mixture made the mixing process more difficult due to the high density and small grain size. In addition, the sand tends to flow preferentially towards the bottom of the container during mixing.

In the samples in which the adhesive was first poured, then the crushed PU waste and sand were added, even with continuous mixing, as a result a strong agglomeration of sand in the mixture was observed. By simultaneous addition of shredded material, sand and the adhesive under constant stirring, we obtained the best results in terms of homogeneity of the material, the strength of the material and the ease of sample detaching from the molds.

**Table 1.** *The quantities of material and parameters used experimentally.*

Sample	PU waste (g)	PU adhesive (g)	Quartz sand (g)
Sample composition: PU waste, PU adhesive Curing temperature: 32°C; Duration of hardening: 4 days			
1	1	4	0
2	3	4	0
3	5	5	0
4	7	5	0
5	10	6	0
Sample composition: PU waste, PU adhesive, quartz sand Curing temperature: 35°C; Duration of hardening: 4 days			
6	2	3	5
7	3	3	7
8	5	4	9
9	6	6	10
10	7	6	11

After removing the hardened samples from the molds, from each sample a small amount of material of about 1 cm<sup>3</sup> was removed and their apparent density were determined (table 2). Next, the samples were immersed in water and kept for 7 and 14 days, to determine the liquid retention (table 2). It was found that with the increase in the amount of waste that was added to the composition, the apparent density also increased. This effect was also assumed to be due to the higher density of the adhesive. Water retention after 7 days is higher for samples with a higher percentage of waste, which is acceptable considering the higher porosity of the material. As expected, the water retention after 14 days is even higher, due to the water-soaking phenomenon of the porous material. After the 14 days, the water retention in the samples becomes insignificant.

**Table 2.** *Apparent density of samples and water retention.*

Sample	Density (g/cm <sup>3</sup> )	Water retention after 7 days (g)	Water retention after 14 days (g)
Sample composition: PU waste, PU adhesive			
1	0.041	0.11	0.19
2	0.065	0.14	0.29
3	0.092	0.27	0.45
4	0.121	0.45	0.55
5	0.158	0.54	0.58
Sample composition: PU waste, PU adhesive, quartz sand			
6	0.258	0.22	0.56
7	0.297	0.33	0.80
8	0.324	0.41	0.84
9	0.407	0.55	0.83
10	0.469	0.62	0.86

## CONCLUSIONS

The experimental study proposed the implementation of a practical solution regarding the recovery of polyurethane waste and its reuse through physical-mechanical methods to obtain a composite material that could be used as an insulating material in constructions. Experimentally, various proportions of materials were used to create samples: PU waste, PU adhesive and quartz sand. The best results were obtained for the samples in which the simultaneous addition of the shredded PU waste and PU adhesive was carried out, under continuous mixing. Samples 3 – 5, which contain a mixture of PU waste and PU adhesive, are similar in appearance, uniformly hardened and homogenous. In samples containing sand, as the amount of sand increases, the homogeneity of the samples decreases. The samples that contain a larger amount of quartz sand show a higher brittleness (samples 9-10).

From an economic point of view, it is preferable to use the mixture of PU waste and fresh PU adhesive instead of fresh PU foam. The mix can use a large amount of PU waste, which can serve as a substitute for fresh PU foam, but requires the addition of PU adhesive, which has a lower cost comparing to PU foams and as a result, the raw material costs decrease considerably.

## REFERENCES

- Böer P., Holiday L., Kang T. H. K., 2014, Interaction of environmental factors on fiber-reinforced polymer composites and their inspection and maintenance: A review. *Construction and Building Materials*, **50**, pp. 209-218.
- Goods S. H., Neuschwanger C. L., Henderson C., Skala D. M., 1997, Mechanical properties and energy absorption characteristics of a polyurethane foam. *Unlimited Release*, pp. 7-35.
- Howarth G. A., 2003, Polyurethanes, polyurethane dispersions and polyureas: Past, present and future. *Surface Coatings International Part B: Coatings Transactions*, **86**, pp. 91-168.
- Kapps M., Buschkamp S., 2004, The production of rigid polyurethane foam. *Bayer Material Science A.G.*, Issue 2004-06-29, pp. 1-46.
- Kojio K., Mutsuhisa F., Yoshiteru N., Nakamura S., 2010, Control of mechanical properties of thermoplastic polyurethane elastomers by restriction of crystallization of soft segment. *Materials*, **3**, pp. 5097-5110.
- Mounanga P., Gbongbon W., Poullain P., Turcry P., 2008, Proportioning and characterization of lightweight concrete mixtures made with rigid polyurethane foam wastes. *Cement and Concrete Composites*, **30** (9), pp. 806-814.
- Priscariu C., 2011, Polyurethane Elastomers - From morphology to mechanical aspects. *Springer Wien-New York*, pp. 231-234.
- Sharmin E., Zafar F., 2012, Polyurethane: An introduction, INTECH Open Access Publisher, pp. 4-15.
- Yang W., Dong Q., Liu S., Xie H., Liu L., Li J., 2012, Recycling and disposal methods for polyurethane foam wastes. *Proceeding Environmental Sciences*, **16**, pp. 167-175.
- Xu T., Yuan W, Wan S., Li Z., Sun B., Wang M., 2008, Synthesis of polyurethane modified bismaleimide (UBMI) and polyurethane-imide elastomer. *Chinese Journal of Polymer Science*, **26** (1), pp. 117-119.
- Zevehoven R., 2004, Treatment and disposal of polyurethane wastes: options for recovery and recycling, Helsinki University of Technology, Report TKK-ENY-19, pp.18-23.



## THE INFLUENCE OF LANDFORM IN THE DISTRIBUTION OF HOUSEHOLDS OF ILVA MICĂ TERRITORIAL ADMINISTRATIVE UNIT

Gheorghe ROȘIAN<sup>1\*</sup>, Csaba HORVATH<sup>2</sup>, Liviu MUNTEAN<sup>1</sup>,  
Nicolae BACIU<sup>1</sup>

<sup>1</sup>*Babeș-Bolyai University, Faculty of Environmental Science and Engineering, Fântânele Street, No. 30, 400294, Cluj-Napoca, Romania*

<sup>2</sup>*Babeș-Bolyai University, Faculty of Geography, Clinicilor Street, No. 5-7, 400006 Cluj-Napoca, Cluj County, Romania*

*\*Corresponding author: gheorghe.rosian@ubbcluj.ro*

**ABSTRACT.** In the case of territorial administrative units located in hilly and mountainous lands, landform, through its morphometric parameters, is a variable that introduces significant differences in the distribution of households. A similar situation is the case of the Ilva Mică commune, where, due to its position at the border between the Eastern Carpathians and the Transylvanian Basin, the landform is extremely varied. Among the parameters of the landform taken into consideration for tracking the distribution of households, the following parameters stand out: altitude, slope and slope aspect. The results show that as the development of Ilva Mică took place, favorable lands were used for building households along with less favorable areas located at altitudes higher than the average altitude of the commune (704 m) and with slopes higher than 17°. This occurred both because of lack of space and of economic reasons, such as the land use for livestock.

**Key words:** *altitude, slope, aspect, household, distribution.*

### INTRODUCTION

The territorial administrative unit of Ilva Mică is located in the north-eastern extremity of the Transylvanian Basin, on the border of Eastern Carpathians. From a regional point of view, it overlaps with the following morphostructural units (figure 1): The Someșan Plateau, the Someșului Mare stream corridor, the Bistrița Hills and the Bârgăului Mountains (Pop, 2001,

2006; Roșian, 2020). Administratively, it belongs to Bistrița Năsăud County, within which it has the rank of commune (figure 1). There is only one village, Ilva Mică, which is commune's residence. There are 3.220 inhabitants grouped in 1.174 households. The territorial administrative unit has a surface area of 2.474 ha.

As a result of a long geomorphological evolution, the landform is complex as a result of a fluvial modelling. Thus, a series of valley corridors were formed which are separated by interfluvial divides. The valley corridors that stand out are Someșul Mare, Ilvei, Leșului and Strâmbei to which are added those of their tributaries. The most significant interfluvial divides are: Ursoiului Hill (between Feldrișelului and Someșului Mare valley), Prislopului Hill (between Someșului Mare and Ilvei valley), the Big Hill (between Ilvei and Leșului valley), Heniu Mountain (between Strâmba and Bârgău valleys) and Băzarnic Peak, between Strâmba and Someșului Mare valley.

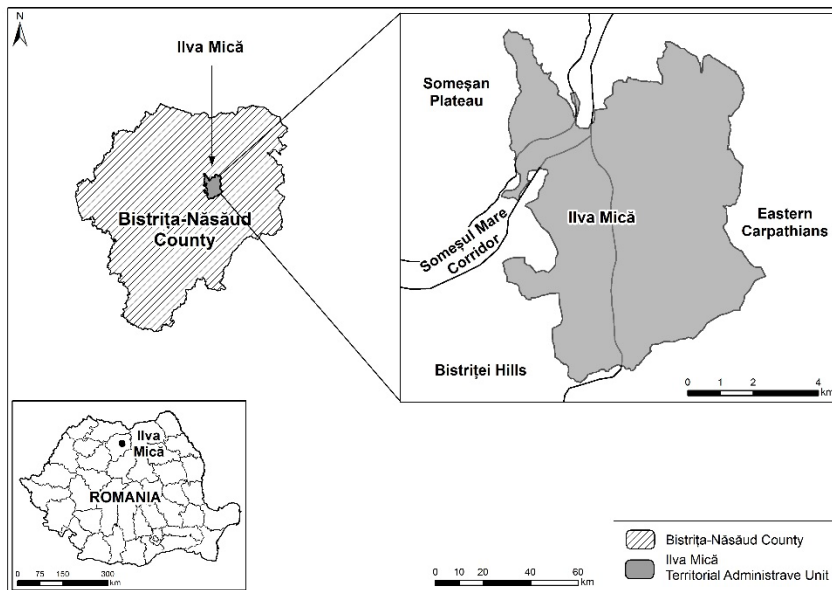


**Fig. 1. Localization of the study area**

The connection between the inferior stream valley corridors and the interfluves is made through steep inclined surfaces, the slopes.

The 400-500 m altitude differences between the upper and lower part of the slopes are a restrictive factor in the proper land use, as well as in the building of transversal roads which ensure an easier connection with neighbouring localities.

Starting from these landform features, in order to follow how it influences the distribution of households, three morphometric parameters have been taken into consideration: altitude, slope and slope aspect.

## **MATERIAL AND METHODS**

To identify the distribution of households based on altitude, slope and aspect, a statistical GIS methodology was used.

Initially, starting from the existing information on topographic maps, the contour lines were vectorised, which, in this case, have a 10 m interval. Using the Esri ArcMap 10.5 software Spatial Analyst extension, with the Topo to Raster Interpolation, a Digital Elevation Model is obtained for the study area. In order to establish the area of the desired altimetric levels, this is run through the reclassification process. Also, the slopes and the aspect are obtained from the same Digital Elevation Model using the Slope and Aspect functions. To identify the value of the areas specific to each altitudinal level, slope or aspect class, the Reclass and Reclassify functions in the Spatial Analyst extension, the Raster to Polygon function in the Conversion Tools extension, and the Summary Statistics function in the Statistics extension were used.

Subsequently, after obtaining the classes of the above-mentioned parameters and their corresponding areas, we assessed the distribution of households in Ilva Mică according to the characteristics of the landform. Households were vectorised based on remote sensing images with the Esri ArcMap 10.5 software Editor function. Both the households in which activities are carried out throughout the year and those with seasonal activities, related to animal husbandry, were vectorised. To identify the distribution of households according to the parameters of the landform, initially a query expression was used, and then a selection was performed based on location.

## **RESULTS AND DISCUSSIONS**

Following the mentioned methodology, it can be noticed that in the case of the Ilva Mică commune, landform is one of the most important variables that introduces variations in the household distribution. All three parameters of the landform (altitude, slope and aspect) have influenced individually, as will be further detailed, the development and evolution of the settlement.

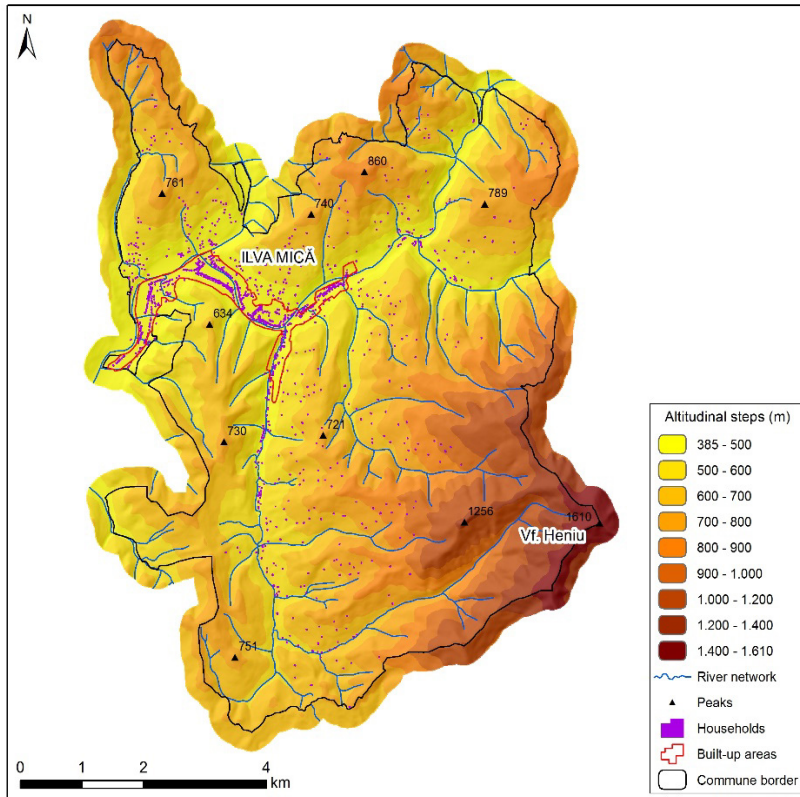


**Fig. 2.** *Distribution of households on altitudinal steps at Ilva Mică*

Altitude is one of the parameters of the landform with the greatest influence in the distribution of human elements on the surface of a territorial administrative unit. This statement is also valid in the case of the household distribution in Ilva Mică. As can be seen in figure 2, the altitude varies between 385 m (in the Someșului Mare corridor) and 1610 m (in Heniu Peak, in the Bârgăului Mountains). The altitudinal difference recorded between these extremities is of 1225 m, while the average altitude is of 704 m.

Of the nine altitude levels chosen for the observation of the household distribution, one can notice that the largest surface corresponds to the 600 and 700 m level (table 1). At the same time, most households are located on the 385 and 500 m altitudinal level even if this is not the largest surface area. Other altitude level favorable to the location of households are the following: 500 - 600 m and 600 - 700 m (table 1).

THE INFLUENCE OF LANDFORM IN THE DISTRIBUTION OF HOUSEHOLDS OF ILVA MICĂ  
TERRITORIAL ADMINISTRATIVE UNIT

**Table 1.** *The surface of the altitudinal steps and the afferent households at Ilva Mică*

Altitudinal steps	Surface (ha)	Weight (%)	Number of households	Weight (%)
385-500	716	13	789	67
500-600	1106	21	162	14
600-700	1407	27	129	11
700-800	936	17	68	5
800-900	442	8	19	2
900-1000	235	4	7	1
1000-1100	359	7	0	0
1200-1400	118	2	0	0
1400-1610	44	1	0	0
Total	5363	100	1174	100

**Table 2.** *The surface of the slope classes and the afferent households at Ilva Mică*

Slope class (°)	Surface (ha)	Weight (%)	Number of households	Weight (%)
0-2	43	1	71	6
2-5	140	3	206	18
5-7	119	2	117	10
7-12	562	10	301	26
12-17	1095	20	278	23
17-22	1105	21	142	12
22-30	1332	25	57	4
30-35	574	11	2	1
35-54	393	7	0	0
Total	5363	100	1174	100

The slope also introduces significant differences in the distribution of households. At Ilva Mică the values of this parameter are between 0° (in the Someşului Mare floodplain) and 54° on the northern slope of Heniu Peak (figure 3); the average slope value is 21°.

Out of the nine chosen classes of slopes on which to follow the household distribution, one can notice that the largest area belongs to the class corresponding to 22 and 30° (table 2). At the same time, most households are specific to the class belonging to 7 and 12°. Even in this case, this slope class does not represent the largest surface area. Other classes favourable to the location of households are the following: 12 - 17°, 2 - 5° and 17 - 22° (table 2).

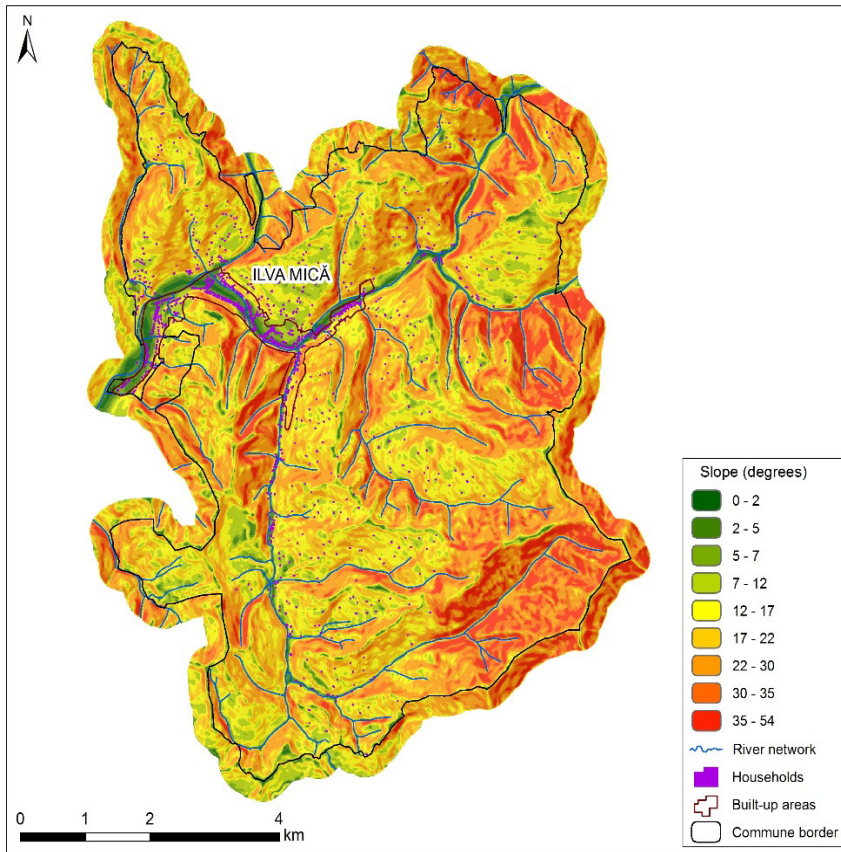


**Fig. 3.** *Distribution of households by slope classes at Ilva Mică*

In turn, the aspect of the areas introduces significant differences in the distribution of households (figure 4). The exposure decisively determines the heat conditions and the humidity of the soil and the substrate, it influences the freeze-thaw cycles, the type and nature of the cover deposits on the hill slopes and it causes qualitative differences in the geomorphological processes preceding erosions (Jakab, 1979).

In the Ilva Mică commune, of the 8 types of aspect, the north western surfaces have the highest value (table 3). At the same time, most of the households are located in the areas exposed to the southwest, because sunny areas are more preferred. Other types of positive slope aspect for the household location are: south, northwest and western slopes (table 3).

THE INFLUENCE OF LANDFORM IN THE DISTRIBUTION OF HOUSEHOLDS OF ILVA MICĂ  
TERRITORIAL ADMINISTRATIVE UNIT

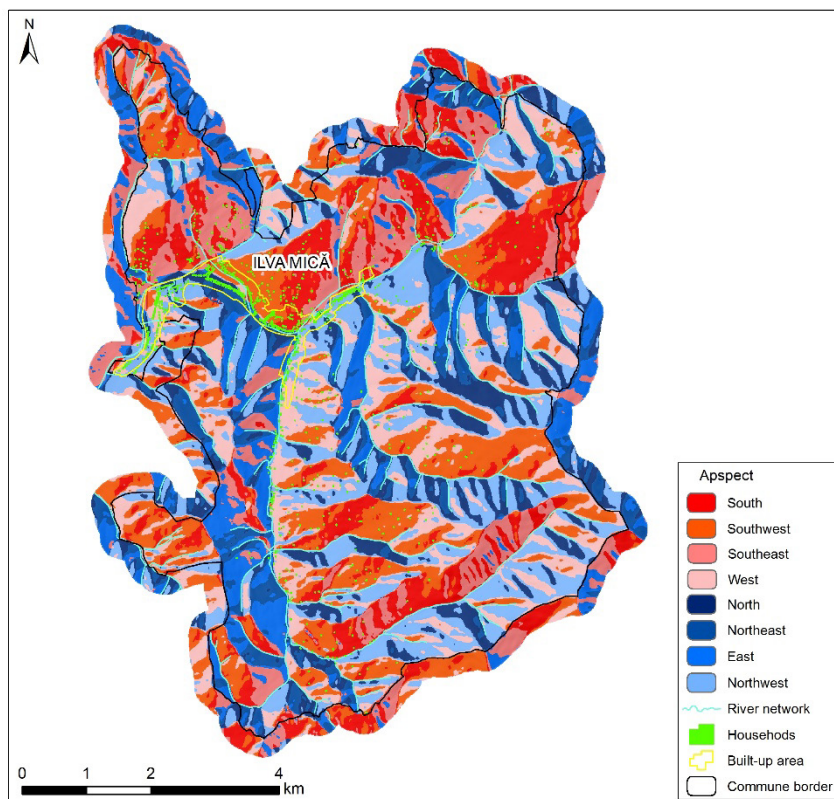


Fig. 4. Distribution of households according to aspect at Ilva Mică

Table 3. The surfaces of slope aspect and the afferent households at Ilva Mică

Types of exposure	Surface (ha)	Weight (%)	Number of households	Weight (%)
South	676	12	219	19
Southwest	932	18	271	23
Southeast	521	10	72	6
West	894	17	195	17
North	505	9	99	8
Northeast	394	7	54	4
East	445	8	55	5
Northwest	996	19	209	18
<b>Total</b>	<b>5363</b>	<b>100</b>	<b>1174</b>	<b>100</b>

It can be noticed from the above that the preferred areas for the location of households in Ilva Mică are those with an altitude between 600 and 700 m, a slope between 7 and 12° and with a southwestern slope aspect.

Based on the above, it can be assumed that in Ilva Mică the households are to be found mainly on three types of landforms: on the low valley corridors, on the hill slopes and on the water divide areas.

Along with the distribution of households, the landform has also influenced the distribution of the street network. The main street has a longitudinal profile that runs on a west-east direction. From this, secondary roads emerged which follow the direction of the river tributaries, running on the north-south direction. Along with these, there are also numerous roads towards the households located on the hill slopes. Such a layout of the street network is primarily due to the various levels and fragmentation of the landform (valley corridors, hill slopes and water divide areas).

At the same time, the horizontal fragmentation of the landform by means of valley corridors, has determined a strong fragmentation of the built-up area in Ilva Mică.

Although, initially, the development and expansion of the built-up area took place on the low valley corridors, later, due to financial constraints and lack of space, the subsequent development included less suitable areas, located on the hill slopes. This situation is specific both to Ilva Mică and to other localities (Petrea, 1998; Gupta and Ahmad, 1999; Roșian et al., 2016; Poszet, 2017).

The fact that on inclined surfaces, such as hill slopes, more and more households were built in the last two decades, it reveals a dangerous trend in the long run, in terms of viability and safety of construction. For this reason, we consider that it is recommended that the extension of the built-up area to take place on surfaces that do not show any susceptibility to geomorphological processes (Dhakal et al., 2000; Bathrellos, 2007) like landslides and eroding riverbanks.

## **CONCLUSIONS**

The emergence and development of Ilva Mică was significantly influenced by the parameters of the landform. Although initially the households were located mainly on favourable lands, on the lower parts of the Someșului Mare and Ilva river corridors, later the number of households increased which included building them up on less favorable areas, such as hill slopes and water divides.

The landform through its parameters (altitude, slope, aspect, etc.) has influenced the building ratio at Ilva Mică. If on the lower part of the valley corridors there are compact buildings, which are part of the built-up area, on the inclined surfaces, like hill slopes, or those located at higher altitudes, like water divides, there are in the vast majority of the cases lonely buildings unincorporated in the built-up area. In the case of the latter, the same anthropic activities are carried out as in the built-up area, with the specification that some of the households are seasonal.

Even if they were analysed separately, there are obvious correlations between the landform parameters. For example, the slope influences both the expansion in height of households and the vertical distribution of buildings. Imposing constructions such as schools, administrative offices, churches or cultural centres are located on low-slope areas, thus avoiding special arrangements, while small individual households are built on hill slopes with slopes higher than  $17^\circ$ .

The presented data show that among the elements of the natural environment, landform has influenced in a specific manner the distribution of households in Ilva Mică. Practically, the unevenness of the landform influenced the spread of the buildings. It can be noticed that the most favourable areas for the household's location in Ilva Mică are those with an altitude between 600 and 700 m, a slope between  $7^\circ$  and  $12^\circ$  and a southwest aspect. Having these in mind, the most unfavourable areas are located at altitudes higher than 1000 m, with an inclination greater than  $30^\circ$  and with a northeast aspect. Thus, the higher the altitude, the slope and the lower the amount of sun energy, the lower the number of households.

## REFERENCES

- Bathrellos G. D., 2007, An Overview in Urban Geology and Urban Geomorphology, Bulletin of the Geological Society of Greece. *Proceedings of the 11th International Congress, Athens, Greece, XXXX*, pp 1335-1337.
- Dhakal A.S., Amada T., Aniya M., 2000, Landslide Hazard Mapping and Its Evaluation using GIS: An Investigation of Sampling Schemes for a Grid-cell Based Quantitative Method. *Photogrammetric Engineering & Remote Sensing*, **66** (8), pp. 981–989.
- Gupta A., Ahmad R., 1999, Geomorphology and the Urban Tropics: Building an Interface between Research and Usage. *Geomorphology*, **31**, pp 133-149.
- Jakab S., 1979, Asimetria versanților din Dealurile Târnavei Mici și ale Nirajului, Trav. Station „Stejarul”. *Geologie-Geografie Series*, **7**, pp. 23-33.

- Petrea R., 1998, Dimensiunea geomorfologică în dezvoltarea și estetica urbană a orașelor mici din Dealurile de Vest (sectorul dintre Barcău și Crișul Negru), University of Oradea Publishinghouse.
- Pop G., 2001, Depresiunea Transilvaniei, Cluj University Press, Cluj-Napoca.
- Pop G., 2006, Carpații și Subcarpații României, 2<sup>nd</sup> edition, Cluj University Press, Cluj-Napoca.
- Poszet S. L., 2017, Studiu de geomorfologie aplicată în zona urbană Cluj-Napoca, Știința Press, Cluj-Napoca.
- Roșian G., 2020, Relieful din Depresiunea Transilvaniei, Universitară Clujeană Press, Cluj-Napoca.
- Roșian G., Maloș C., Muntean O. L., Mihăiescu R., Dobrei G., 2016, Geomorphological Constraints in the Urban Development of the Gruia District in Cluj-Napoca. *Studia - Ambientum*, **61** (1-2), pp 119-127.

# CHEMICAL CHARACTERISATION OF ACID MINE DRAINAGE FROM VALEA ŞESEI TAILING DAM (NW OF ROMANIA) AND ITS IMPACT ON SURFACE WATER QUALITY

Diana Iuliana TOMUŞ<sup>1</sup>, Carmen ROBA<sup>1\*</sup>, Cristina ROŞU<sup>1\*</sup>

<sup>1</sup>*Babeş-Bolyai University, Faculty of Environmental Science and Engineering,  
30 Fântânele Street, Cluj-Napoca, Romania*

*\*Corresponding authors: cristina.rosu@ubbcluj.ro; carmen.roba@ubbcluj.ro*

**ABSTRACT.** The acid mine drainage (AMD) can be a major source of water and soil pollution. To evaluate the chemical composition of the AMD and its impact on surface waters, a total of 132 water samples, both surface and waste waters, were collected during four field campaigns in November 2018, December 2018, March 2019 and April 2019. There were also collected several samples from the tailing dam material and sediments from the rivers where acidic waters are discharged. The physico-chemical parameters (pH, redox potential, electrical conductivity, total dissolved salts and salinity) were measured by a portable multiparameter (WTW multi350i, Germany), while the dissolved ions ( $\text{NO}_2^-$ ,  $\text{NO}_3^-$ ,  $\text{Br}^-$ ,  $\text{F}^-$ ,  $\text{Cl}^-$ ,  $\text{PO}_4^{3-}$ ,  $\text{SO}_4^{2-}$ ,  $\text{Li}^+$ ,  $\text{Na}^+$ ,  $\text{NH}_4^+$ ,  $\text{K}^+$ ,  $\text{Mg}^{2+}$  and  $\text{Ca}^{2+}$ ) were analysed by ion chromatography and the metal content (Cu, Zn, Fe, Cr, Cd, Ni, Pb) was determined by atomic absorption spectrometry. Most of the water samples had an acidic pH, with high electrical conductivity values (up to 9,360  $\mu\text{S}/\text{cm}$ ). The waters had a high level of  $\text{SO}_4^{2-}$  (up to 8141.8 mg/l), Fe (up to 1,216.2 mg/l), Cu (up to 71.9 mg/l) and Zn (up to 61.98 mg/l). The tailing dam material was characterised by high levels of Fe (39.87 – 40.72 g/kg), Zn (81.3 – 241.1 mg/kg), Cu (343.5 – 942.3 mg/kg) and Pb (41.4 – 77.1 mg/kg). The analyses indicated the negative impact of AMD discharge in surface waters, which proved to have high levels of  $\text{SO}_4^{2-}$  and heavy metals.

**Key words:** *acid mine drainage, heavy metals pollution, tailing dam, Valea Şesei.*

## INTRODUCTION

Mining activities represents a major source of pollution for the environment, generating pollutants, like heavy metals, which can have a significant negative impact on the environment and human health (Hadzy et

al., 2015; Islam et al., 2015; Linkuku et al., 2013). Roșia Poieni (Alba County) is the largest copper ore exploitation from Romania and the second largest in Europe, consisting of more than a billion tonnes of porphyry-type ore, with an average of 0.36% Cu (Milu et al., 2002; 2004; Rzymiski et al., 2017). The exploitation of the copper ore is carried out in the open pit manner and all the generated wastes are deposited at Valea Șesei tailing pond, situated on the valley with the same name, which is the right affluent of Arieș River (figure 1). The dam is built from limestone blocks and gravel and it has a height of 118 m and an inclination of 33° (Duma, 1998; Melenti et al., 2011). Downhill from the dam, at approximately 1.2 km, is the confluence between Valea Șesei and Arieș River (Melenti et al., 2011). The acid mine drainage (AMD) generated by the tailing pond, can be a major source of water and soil pollution in the area.

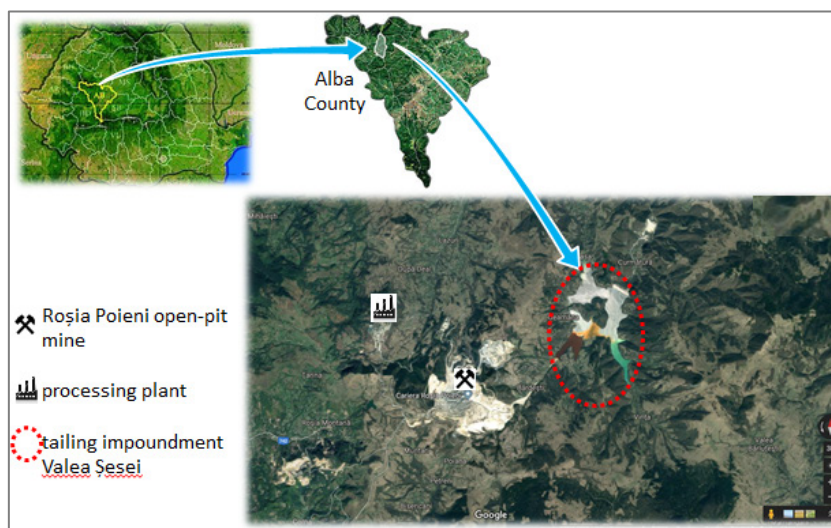


**Fig. 1.** Location of Valea Șesei tailing impoundment

The main purposes of the present study were: (1) to evaluate the chemical composition of sterile deposited on the tailing impoundment; (2) to evaluate the chemical composition of wastewaters generated by the tailing impoundment; (3) to evaluate the impact of acidic mine drainage (AMD) on surface water downstream from Roșia Poieni mine and (4) to assess the seasonal fluctuation of chemical parameters.

Similar studies have been conducted in the area, like the ones performed by Melenti et al. (2011), Milu et al. (2002, 2004), Rzymiski et al. (2017), or Ștefănescu et al. (2010).

## MATERIALS AND METHODS

A total of 12 sterile samples were collected during November 2018 and March 2019, from six sampling points: S1 – S5 (tailing impoundment) and S6 (tailing pipe). Supplementary, 132 water samples were collected in triplicate, during November 2018, December 2018, March 2019 and April 2019. The water samples consisted of surface waters from Valea Holhorii creek (SW1), Valea Şesei creek (SW2 – SW8), Arieş River (SW9 – SW10) and wastewaters (W1 – W6).

The investigated physico-chemical parameters (pH, Eh – redox potential, EC – electrical conductivity, TDS – total dissolved salts and salinity) were measured using a portable multiparameter (WTW Multi 350i). In the case of water samples, these parameters were measured *in situ*, while for sterile samples they were measured in the laboratory, after the extraction with distilled water (ratio 1:5) (SR 7184-13/2001; Mofor et al., 2017).

The water samples used for the analysis of major dissolved ions ( $F^-$ ,  $Cl^-$ ,  $Br^-$ ,  $NO_2^-$ ,  $NO_3^-$ ,  $PO_4^{3-}$ ,  $SO_4^{2-}$ ,  $Li^+$ ,  $Na^+$ ,  $K^+$ ,  $NH_4^+$ ,  $Mg^{2+}$ ,  $Ca^{2+}$ ) were filtered (0.45  $\mu m$ ), kept in the refrigerator (at dark and 4°C) and analysed using an ion chromatograph system (Dionex 1500 IC, USA).

The heavy metals (Pb, Fe, Zn, Ni, Cd, Cu, Cr) analyses were performed by atomic absorption spectrometry (AAS), by using a ZEE nit 700 system (Analytik Jena) equipped with air – acetylene burner, a graphite furnace, and a special hollow – cathode lamp for each metal. Before AAS analyses, the soil samples were dried in oven at 105°C for 24 hours, ground and sieved through 250  $\mu m$  sieve, then were mineralized with *aqua regia* overnight at room temperature, then heated to reflux on sand bath for 2 h, filtered (0.45  $\mu m$ ) and diluted to 100 ml with  $HNO_3$  (0.5%). The water samples were acidified at a  $pH \approx 2$  with  $HNO_3$  (65%) and filtered (0.45  $\mu m$ ).

## RESULTS AND DISCUSSIONS

### Sterile samples

The results for the analysed physico-chemical parameters (figure 2) indicated the heterogenic character of the analysed samples. The sterile from sampling points S2 and S3 proved to be acidic, while the rest of the samples had an alkaline pH. The acidic nature of samples S2 and S3 is a consequence of the location of these two sampling points in the vicinity of the acid mine

drainage inflowing from Roșia Poieni copper mine to Valea Șesei. The rest of the samples had an alkaline pH, because they were samples close to the pipe which transports sterile and wastewaters from processing plant, which uses lime as flotation reagent and from the vicinity of the pipe which transports slaked lime for neutralization.

Samples S2 and S3 proved to have the highest EC and salinity, reflecting the high amounts of salts. The seasonal fluctuations indicated that the pH and Eh levels were generally higher during March 2019, while the EC and salinity were higher during November 2018, comparing to March 2019 (figure 2).

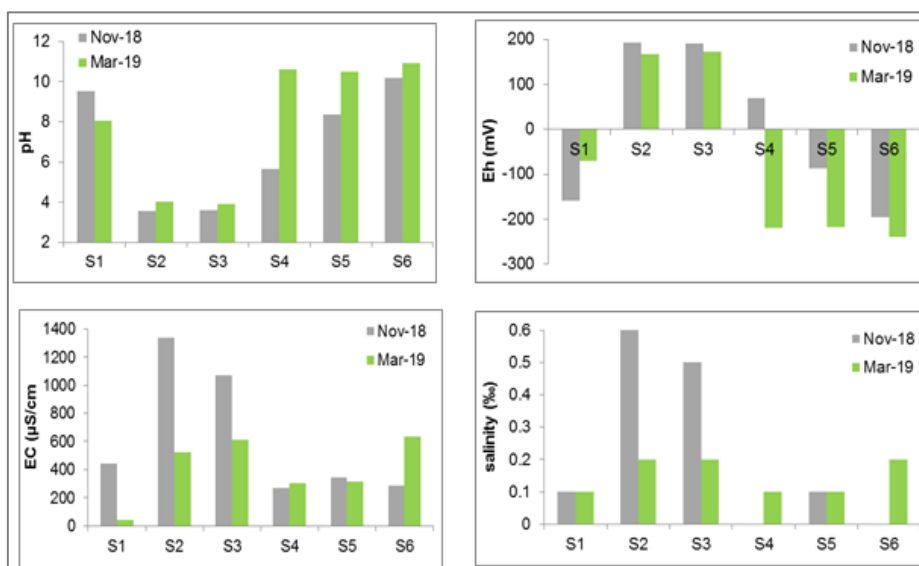


**Fig. 2.** The physico-chemical parameters of the sterile samples

The metals distribution in sterile samples was dominated by the presence of Cu (278 – 942 mg/kg), Zn (48 – 230 mg/kg) and Pb (23 – 77 mg/kg), which had higher concentrations than Cr (2 – 10 mg/kg), Ni (2.6 – 6.9 mg/kg) and Cd (1.3 – 2.2 mg/kg) (Fig 3). The highest concentrations were registered in S6 point, where the sterile and waste water are discharged.

Generally, the average levels were slightly higher in November 2018 than during March 2019 (figure 3).

CHEMICAL CHARACTERISATION OF ACID MINE DRAINAGE FROM VALEA ŞESEI TAILING DAM (NW OF ROMANIA) AND ITS IMPACT ON SURFACE WATER QUALITY

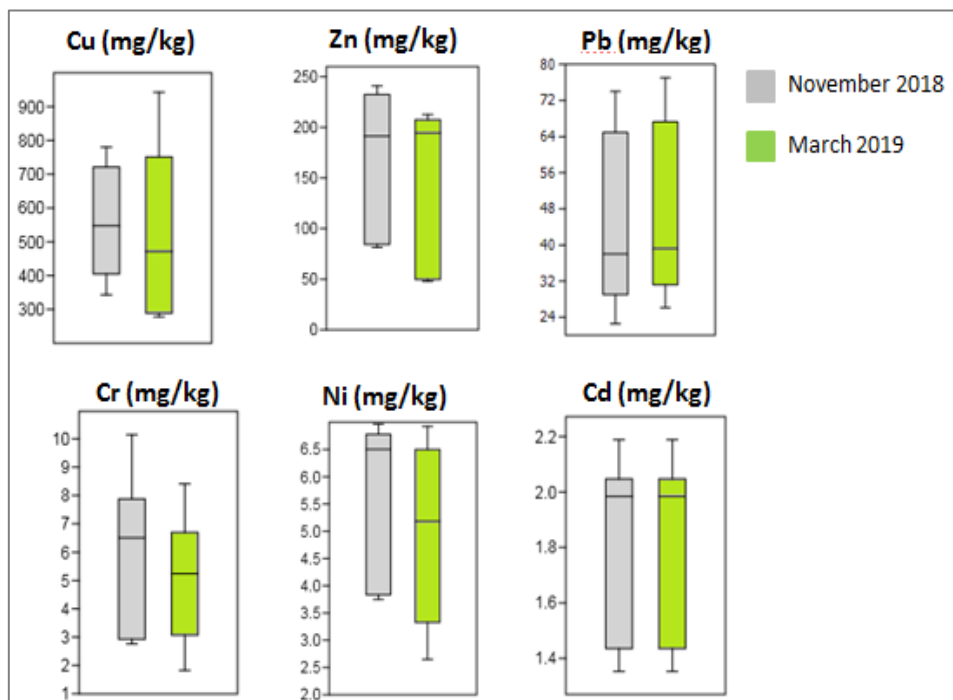


Fig. 3. Seasonal fluctuation of metals content in sterile samples

To have an over role image of the quality of the sterile samples, there were calculated two specific indices: Enrichment factor (EF) and Geo-accumulation index ( $I_{geo}$ ). Enrichment factor was calculated based on the method proposed by Sinex and Helz (1981), using iron as reference metal:

$$EF = \frac{\frac{C_n}{C_{Fe}} \text{sterile}}{\frac{C_n}{C_{Fe}} \text{crust}}$$

where,  $C_n$  is the heavy metal concentration (mg/kg) in sterile and in the upper continental crust, while  $C_{Fe}$  is the iron concentration in both sterile and in the upper continental crust (mg/kg).

Based on EF level, the sterile samples can be classified in five quality classes as follows: unpolluted ( $0 < EF < 1$ ), minor polluted ( $1 < EF < 3$ ), moderate polluted ( $3 < EF < 5$ ), moderately to severe polluted ( $5 < EF < 10$ ), severe polluted ( $10 < EF < 25$ ) and very severe polluted ( $25 < EF < 50$ ) (Simex and Helz, 1981).

Geo-accumulation index, was calculated based on the formulae proposed by Muller (1981):

$$I_{geo} = \ln \frac{C_n}{1.5 \cdot B_n}$$

where,  $C_n$  is the concentration (mg/kg) of heavy metal in sterile sample,  $B_n$  is the concentration (mg/kg) of heavy metal in the upper continental crust and 1.5 is the correction factor.

By calculating  $I_{geo}$ , the sterile samples can be classified as: unpolluted ( $I_{geo} \leq 0$ ), unpolluted to moderately polluted ( $0 < I_{geo} < 1$ ), moderately polluted ( $1 < I_{geo} < 2$ ), moderately to heavily polluted ( $2 < I_{geo} < 3$ ) and heavily polluted ( $3 < I_{geo} < 4$ ).

The values of the calculated indices are presented in figure 4 and figure 5. The results indicated that based on EF values, the analyzed sterile samples are unpolluted with Ni, Cr, minor polluted with Pb, Zn, Cd, moderate polluted with Pb and severe to very severe polluted with Cu (Fig. 4). These results were confirmed by calculating the  $I_{geo}$ , which indicated that the investigated sterile samples are unpolluted with Ni and Cr, unpolluted to moderately pollute with Pb, Cd, Zn, and moderately to heavily polluted with Cu (figure 5).

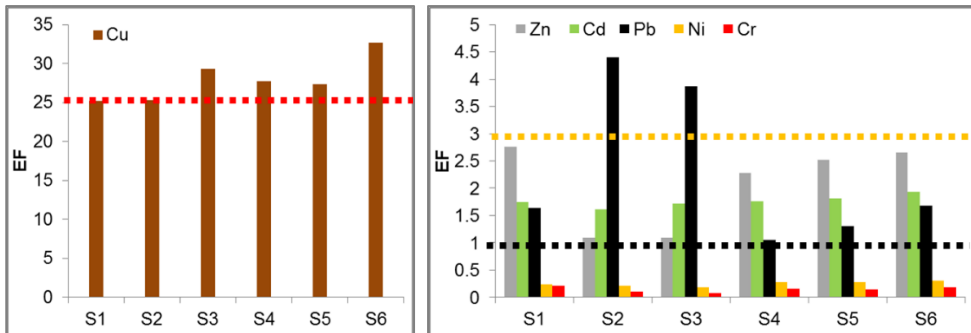


**Fig. 4.** Heavy metals pollution degree of sterile samples, based on the Enrichment Factor (EF) values (unpolluted  $0 < EF < 1$ , minor polluted  $1 < EF < 3$ , moderate polluted  $3 < EF < 5$ , moderately to severe polluted  $5 < EF < 10$ , severe polluted  $10 < EF < 25$  and very severe polluted  $25 < EF < 50$ )

CHEMICAL CHARACTERISATION OF ACID MINE DRAINAGE FROM VALEA ŞESEI TAILING DAM (NW OF ROMANIA) AND ITS IMPACT ON SURFACE WATER QUALITY

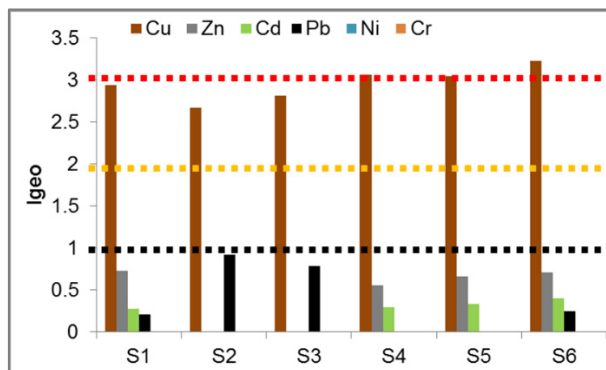


**Fig. 5.** Heavy metals pollution degree of sterile samples, based on Geo-accumulation index ( $I_{geo}$ ) values (unpolluted  $I_{geo} \leq 0$ , unpolluted to moderately polluted  $0 < I_{geo} < 1$ , moderately polluted  $1 < I_{geo} < 2$ , moderately to heavily polluted  $2 < I_{geo} < 3$ , heavily polluted  $3 < I_{geo} < 4$ )

### Water samples

The monthly fluctuation of the physico-chemical parameters for the analysed water samples is presented in Fig. 6. The waste waters sampled from points W3 – W5 proved to be highly acidic, exceeding the limits (6.5 – 8.5) imposed by national legislation (GD 352/2005) for the discharge of waste waters into surface waters. Generally, the waste waters sampled from sampling points W1, W2 and W 6 were alkaline, because they were sampled from the pipe which transports lime for neutralisation and from the pipe which that transports sterile and wastewaters from the processing plant, where lime is used as flotation reagent. The data reflected the impact caused by the discharge of acidic waste waters onto the surface waters, most of them being more acidic than the national recommendations (Order 161/2006) (figure 6).

The waste waters sampled from points W3 – W6 had a high EC and salinity, which reflects the high amounts of dissolved salts. The discharge of these waters into surface waters leads to high levels of EC and salinity for Valea Holhorii creek (SW1) and Valea Şesei creek (SW2 – SW8); only the high dilution with Arieş River (SW9 – SW10) decreases the levels of EC and salinity.

The monthly fluctuation showed that the waters were generally more acidic during April 2019 than in March 2019, while the EC and salinity were slightly higher during April 2019 than in March 2019. These fluctuations can be correlated with the high amounts of precipitations from April 2019.

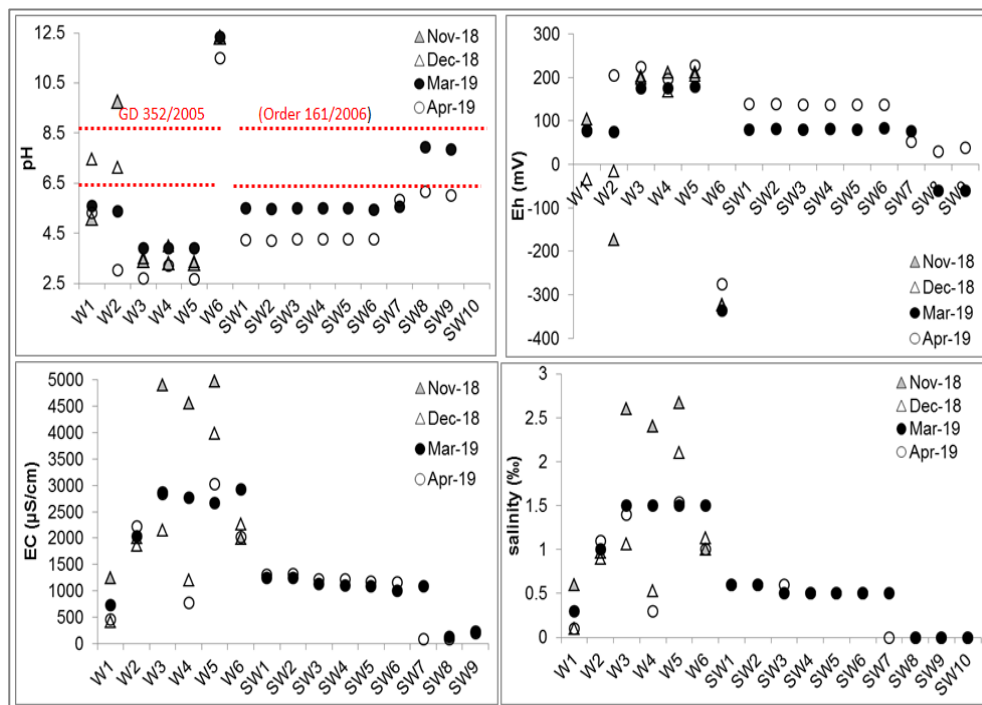


**Fig. 6.** Monthly fluctuation of the physico-chemical parameters for the analysed water samples

The analysed waters proved to have high levels of calcium, magnesium and sulphates, for waste waters these parameters exceeded the limits imposed by national legislation for their discharge into surface waters (figure 7). As a consequence, the discharge of these waste waters had a negative impact on the quality of surface waters, which due to the high content of  $\text{SO}_4^{2-}$ ,  $\text{Ca}^{2+}$  and  $\text{Mg}^{2+}$ , can be classified as having a bad or poor ecological status (S 1 – 7) (Order 161/2006). The content of sodium, potassium, chloride and nitrate, proved to be considerably lower than the other ions (figure 7).

CHEMICAL CHARACTERISATION OF ACID MINE DRAINAGE FROM VALEA ŞESEI TAILING DAM (NW OF ROMANIA) AND ITS IMPACT ON SURFACE WATER QUALITY

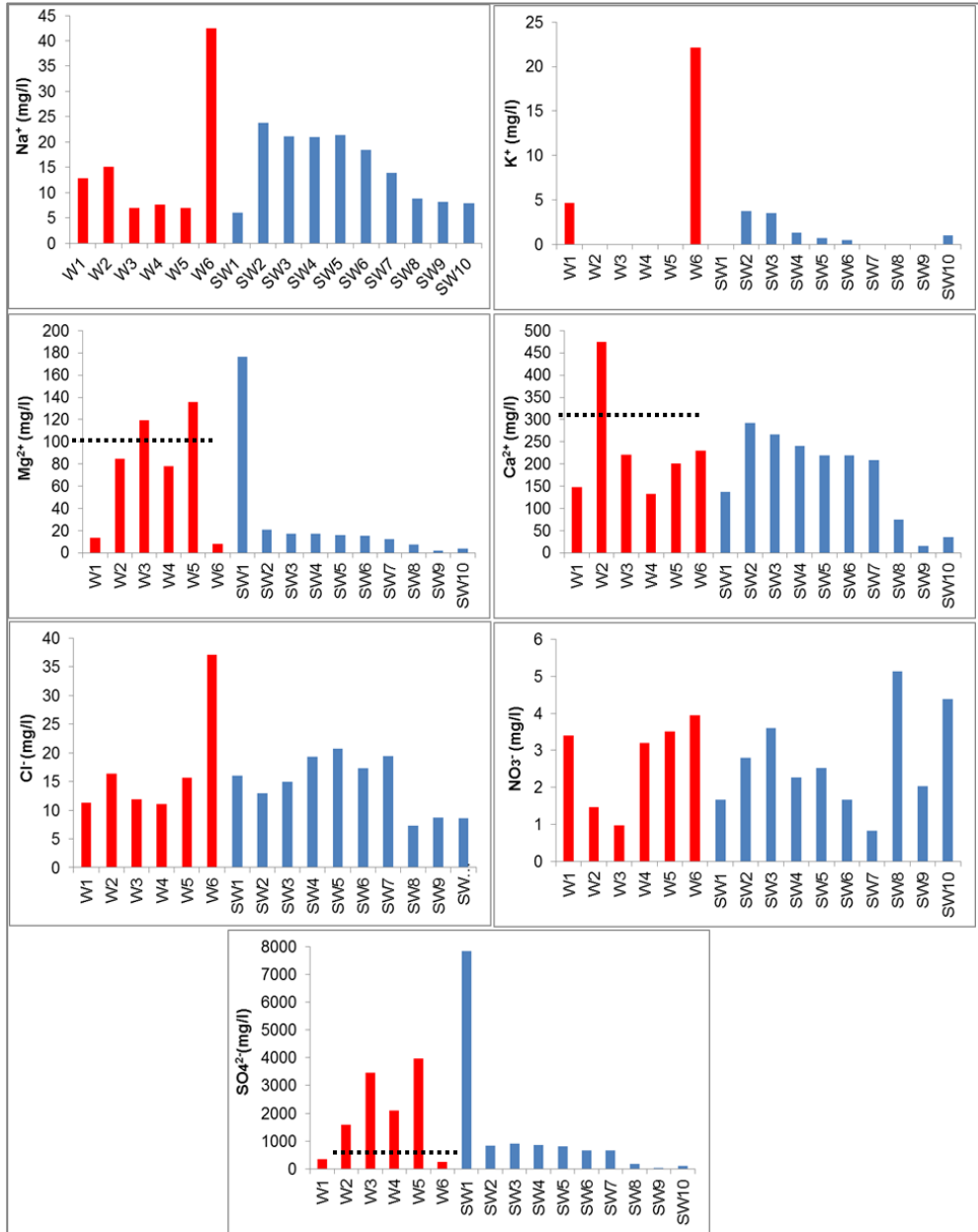


Fig. 7. The content of dissolved ions in both waste waters and surface waters

The waste waters proved to be highly contaminated with copper and zinc, having values (1.7 – 45.6 mg/l, for Cu and 0.1 – 18.7 mg/l for Zn) considerably higher than the maximum permissible limit (MPL) (0.1 mg/l for Cu and 0.5 mg/l for Zn) imposed by national legislation for waste water discharge into surface waters (GD 352/2005). The content of Pb and Cd were close to the MPL, while the content of Cr and Ni were lower than the national legislation requirements.

Consequently, the discharge of wastewater into Valea Holhorii creek (SW1) and Valea Șesei creek (SW2 – SW8) has led to their contamination with heavy metals. Based on Cu, Zn, Pb and Cd content, the surface waters sampled from S1 – S8 points correspond to a bad ecological status (figure 8). Only the high dilution with Aries River decreases the content of heavy metals corresponding to a very good to moderate ecological stats.

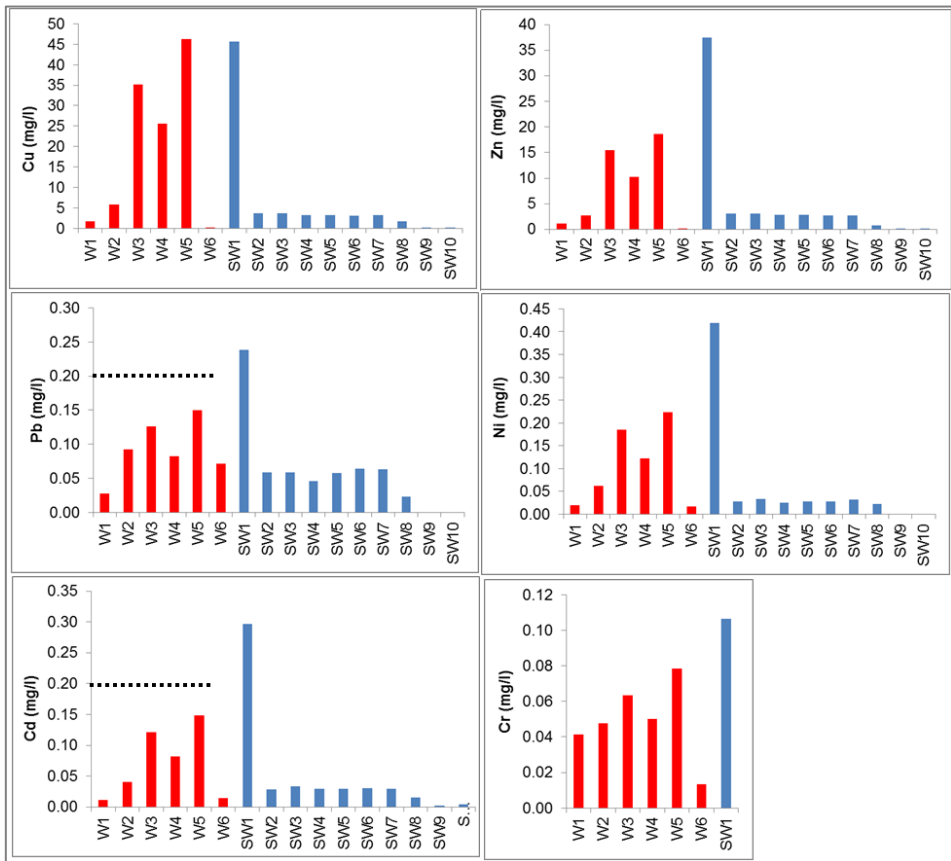


Fig. 8. The content of metals in both waste waters and surface waters

## CONCLUSIONS

The results of the present study showed that the tailing dam material is characterised by high levels of Cu. Tailing impoundment from Valea Şesei represent a high risk for Cu contamination for soil and surface water.

The wastewaters deposited along with tailings in Valea Şesei represent a serious environmental and health risk, containing significant levels of copper, zinc and sulphates.

The analyses indicated the negative impact of AMD discharge in surface waters, which proved to have high levels of Cu, Zn and  $\text{SO}_4^{2-}$ .

## Acknowledgments

We are grateful for the financial support from the Babeş-Bolyai University, during the special student's scholarships (36.040/28.11.2018).

## REFERENCES

- Duma S., 1998, Geoecological study of mining operations in the southern area of the Apuseni Mountains, Poiana Ruscă Mountains and Sebes Mountains. Ed Dacia, Cluj-Napoca, 379 p (in Romanian).
- GD 352/2005, Government Decision regarding the modification and completion of Government Decision no. 188/2002 for the approval of some norms regarding the conditions of discharge in the aquatic environment of waste water.
- Hadzy G.Y., Essumang D.K., Adjei J.K., 2015, Distribution and Risk Assessment of Heavy Metals in surface water from Pristine environments and major mining areas in Ghana. *Journal of Health & Pollution*, 5 (9), pp. 86-93.
- Islam M.S., Ahmed M.K., Raknuzzaman M., Al-Mamun M.H., Islam M.K., 2015, Heavy metal pollution in surface water and sediment: A preliminary assessment of an urban river in a developing country. *Ecological Indicators*, 48, pp. 282-291.
- Linkuku A.S., Mmolawa K.B., Gaboutloeloe G.K., 2013, Assessment of Heavy Metal Enrichment and Degree of contamination around the Copper-Nickel mine in the Selebi Phikwe region, eastern Botswana. *Environment and Ecology Research*, 1. (2), pp. 32-40.

- Melenti I.L., Magyar E., Rusu T., 2011, Heavy metals analysis in waste watersamples from Valea Sesei tailing pond. *Air and water components of the environment*, pp. 539-544.
- Milu V., Leroy J.L., Peiffert C., 2002, Water contamination downstream from a copper mine in the Apuseni Mountains, Romania. *Environmental Geology*, 42, pp. 773-782.
- Milu V., Milesi J.P., Leroy J.L., 2004, Rosia Poieni copper deposit, Apuseni Mountains, Romania: advanced argillic overprint of a porphyry system, *Mineralium Deposita*, 39, pp. 173-188.
- Mofor N.A., Tamungang E.B.N., Mvondo-zé A.D., Kome G.K. and Mbene K., 2017, Assessment of physico-chemical and heavy metals properties of some agricultural soils of Awing-North West Cameroon. *Archives of Agriculture and Environmental Science*, 2, pp. 277-286.
- Muller G., 1981, Die Schwermetallbelastung der sedimente des Neckars und seiner Nebenflüsse: eine Bestandsaufnahme, *Chem. Ztg*, 105, pp. 157-164.
- Order 161/2006, Order of the Ministry of Environment and Water Management (Romania) for the approval of the Norm regarding the classification of surface water quality in order to establish ecological state of water bodies
- Rzymski P., Klimaszuk P., Marszelewski W., Borowiak D., Mleczek M., Nowiński K., Pius B., Niedzielski P., Poniedziałek B., 2017, The chemistry and toxicity of discharge waters from copper mine tailing impoundment in the valley of the Apuseni Mountains in Romania. *Environ. Sci. Pollut. Res.*, 24, pp. 21445-21458.
- Simex S.A., Helz G.R., 1981, Regional geochemistry of trace elements in Chesapeake Bay. *Environ. Geo.*, 3, pp. 315-323.
- SR 7184-13/2001 Soils. Determination of pH in water and saline suspensions (mass/volume) and in saturated paste.
- Stefănescu L., Costan C., Ozunu A., 2010, Risks Associated to Structural Stability of Tailing Dams in the Aries Middle Basin. *ProEnvironment*, 3, pp. 414-423.

# THE QUANTITATIVE AND QUALITATIVE PARAMETERS OF THE BODOC SPRINGS

Melinda VIGH<sup>1\*</sup>

<sup>1</sup>*Babeş-Bolyai University, Faculty of Environmental Science and Engineering,  
30 Fântânele Street, Cluj-Napoca, Romania  
\*Corresponding author: melinda.vigh@ubbcluj.ro*

**ABSTRACT.** The post-volcanic phenomena in the Bodoc area are part of the alignment that flanks the western strip of the Carpathian Chain. The fragmented geological structure facilitated the migration of water and gas to the surface. The characteristics of spring water have been studied since the 19<sup>th</sup> century. On the outskirts of the Bodoc village there are several springs, the most important are Matild, Lenes and Geza. The analysis of water samples was performed in the field (the main parameters) and in the laboratory (major ions). The main water parameters determined in situ where: pH, redox potential, temperature, electrical conductivity, total dissolved solids and salinity, and in the laboratory, where determined the following ions: sodium, calcium, magnesium, ammonia, potassium, lithium, fluorides, chlorides, bromides, nitrites, nitrates, phosphates, sulphates, bicarbonates. The analysis of the parameters shows many similarities, because the springs have the same source or neighbouring sources. At the same time, differences were identified in the case of some parameters, which occurred due to the influence of local factors.

**Key words:** *spring, post-volcanic phenomena, mineral water, spring flow, physico-chemical parameters.*

## INTRODUCTION

### Geology

The geological evolution and structure of the area is complex. The emergence of the Carpathian Mountains began in the Mesozoic and continued into the Paleogene. Then, by folding the more friable sediments, was formed the flysch structure. These processes led to the formation of the Bodoc Mountains, where sandstones, conglomerates, marls and clays dominate (Kisgyörgy and Dukrét, 2001).

The structure is characterized by a sequence of anticlines - synclines orientated on the N - S direction. In the depths are hidden a series of horsts and grabens, of which in the studied area are characteristic the Bicsad - Sfântu Gheorghe graben and the Bodoc horst (Airinei and Pricăjan, 1972). To the east stretches a thrust sheet, to the north appears the Harghita area with volcanic eruptions, and to the south are successive blocks of flysch in the form of steps. For the studied area, the Ceahlău thrust sheet is characteristic, consisting of sandstone facieses. Striped clays and friable alluvial sediments have been deposited along the Neogene sandstones along the valleys.

The whole area is characterized by a strong fragmentation. In the western part of the Bodoc Mountains there are two elongated, almost parallel faults, which start in the volcanic area and cross the flysch. These faults facilitated the frequent occurrence of post-volcanic phenomena (Harkó, 1970), see figure 1.

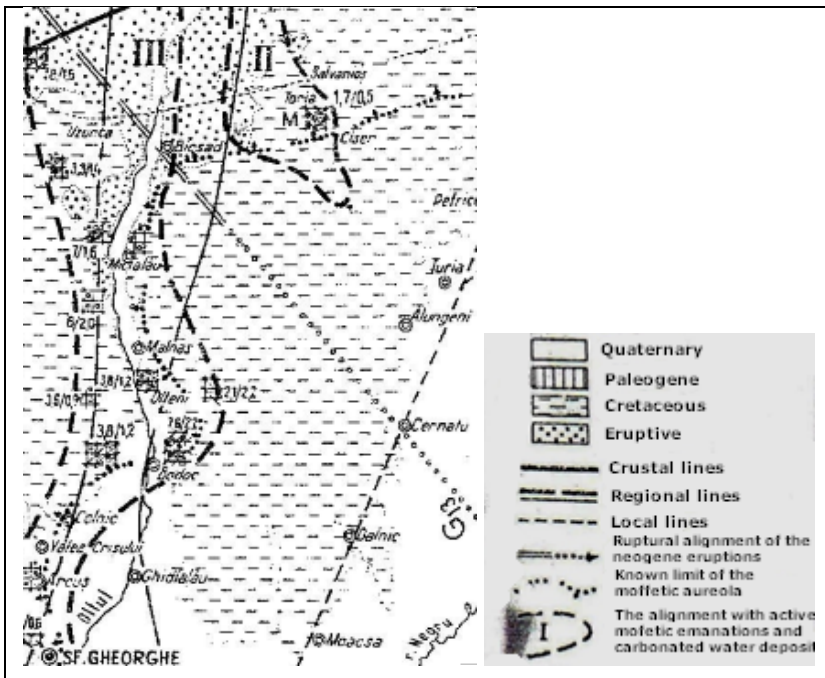


Fig. 1. Geological structure of the area (after Airinei and Pricăjan, 1972)

### Post volcanic phenomena

The area belongs to a vast mofette aureole located in the flysch formations and Neogene-Quaternary deposits. The post-volcanic manifestations have their origin in the Neogene volcanic activity in the volcanic chain of the

Carpathians Mountains. Dry emanations in the form of mofettes and mineral springs can be distinguished, as a result of the mixture of water in its ascending path among the geological structures with the carbon dioxide of the mofettes. The chemical load of spring water differs depending on the composition of the layers of contact rocks crossed. Thus chloro-sodium, ferruginous, sulphated, chlorinated etc. springs appeared.

### **Bodoc Deposit**

The springs in the area Bodoc are located on the slopes and at the foot of the mountains with the same name, in the eastern part of the commune. The famous traveller and explorer of Transylvania - Orbán Balázs, in his pilgrimages from the 19<sup>th</sup> century remarked: "at the end of the village, in the valley of the Borviz brook, there is the famous mineral water, which, bottled, reaches Bucharest" (Orban, 1982). There are several sources, the most important are Matild, Géza and Lenes. The first scientific presentation of the waters in the area was made by Hankó Vilmos at the end of the 19th century (Hankó, 1887). 80 years later, Harkó József publishes the first scientific description of these sources (Harkó, 1970). A few years later, Airinei and Pricăjan carried out an extensive study on the mofette aureole in Covasna County, with considerations on the mineral waters from Bodoc. They specify that the post-volcanic activity at Bodoc belongs to the central alignment of the mofette and mineral water deposits area. It extends north to Bicsad - Tuşnad, as well as south to Sfântu Gheorghe (Airinei and Pricăjan, 1972).

The springs are fed by the hydro mineral accumulation located in the internal unit of the Carpathian flysch – Ceahlău sheet. In the post-tectonic depression Braşov - Târgu Secuiesc there are two aquifers - one groundwater accumulation, poorly mineralized, and one deep, with high mineralization. The latter is confined to sandstone-conglomerate and sandstone-marl-clay deposits. The migration to the surface of deep deposits is facilitated by the existence of cover faults that furrow the area (Bandrabur and Slăvoacă, 1973).

According to the hydrogeological drilling carried out by the ISP in 1962 and Harkó's study, four hydrogeological complexes were identified:

- a groundwater complex, at a depth of 4.5-9.5 m
- a complex rich in carbon dioxide, between 9.5-16 m
- two deep complexes, located between 20-34 m (Harkó, 1970).

### **Matild Spring**

Matild Spring is the most representative and important source in the area. It is located in the north - eastern part of the village, at an altitude of 594 m. It has been known since the end of the 17th century. It is owned by the

village and by the Reformed church. In 1872 it was improved by deepening the spring, equipping it with drainage and building a wooden shelter. It is significant that from the first benefits of capitalizing on water, the village paid a schoolteacher. The Public ownership of the mineral water in Bodoc was then established.

From 1898, the entrepreneur György József started the commercial exploitation of the water from the Matild spring, transporting water by cart to Sfântu Gheorghe, Braşov and Sighişoara, but it reached Vienna and even overseas, where it was very successful (Kisgyörgy, 2008). The first bottling unit was established in 1894 and it operated until 1963 (Feru, 2012). In 1896, at an exhibition that took place in Bucharest, Matild mineral water obtained the gold medal from King Carol I. On this occasion, Victor Babeş also performed chemical analyses on this water. At the Szekler Exhibition of 1905, the mineral water is again awarded the gold medal. During this period, 1500 labelled bottles are already bottled daily, which present the analyses of Hankó and Babeş. In 1922 the Saxon merchant Fleischer rented the spring, from Braşov. The bottling plant is being modernized and increasing its capacity, reaching 6000 bottles in 1948. At the beginning of the 20th century, the original name was changed to Clotild, but it was returned to Matild after 1989. Between 2013-2019, water bottling was stopped. There are currently limited quantities of bottled water on the market.

A hydrogeological drilling was carried out near the Matild spring, under the name Source F 13 RAMIN. Both Matild and F 13 are captured and the water is capitalized through bottling (see in figure 2 the used labels).

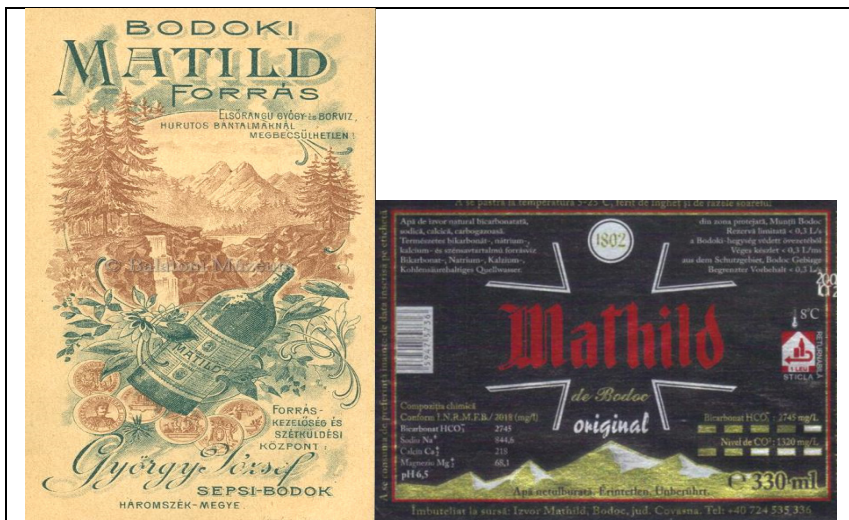


**Fig. 2.** The first and current label of Matild bottled mineral water (<https://mandadb.hu> and <https://izvor.ro>)

### **Lenes Spring**

It is located in a garden called Lenes, whence its name. It is much closer to the village, at the foot of the mountains, at an altitude of 551 m. Near the spring there was once a bath called "Veresfürdő / Red Bath". Orbán Balázs, in "The description of the Szeklerland", mentions the following about this bath: "Above this spring is the Red Bath, which is used for bathing: it's name comes from the colour of the red deposits, it has beneficial effects for colds and gout" (Orbán, 1982).

### **Géza Spring**

It is mentioned in the Sfântu Gheorghe newspaper as one of the two twin springs, which are located on the western slopes of the Bodoc Mountains (Kisgyörgy, 2008). It is located in the east part of the town, at an altitude of 674 m. It is named after a local enthusiast, who for a long time took care of this spring. It looks like a burst, around which a concrete ring has been built.

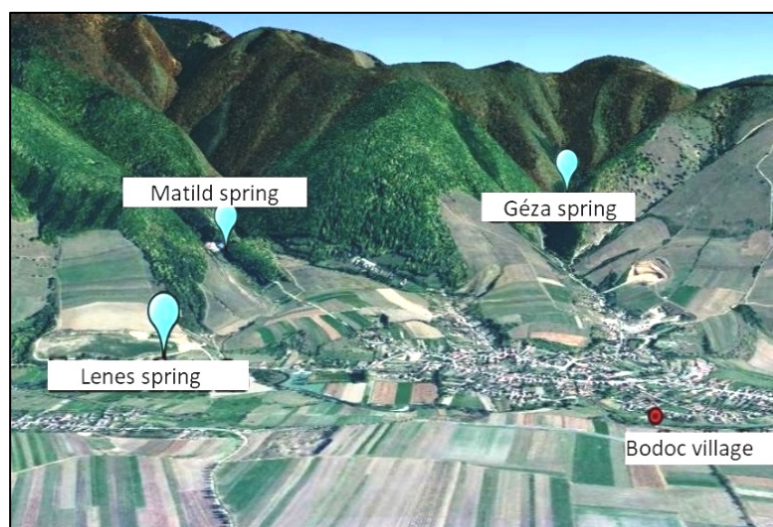


**Fig. 3.** Location of the springs

## **METHODOLOGY**

The field activity consisted of collecting samples in half-litter bottles, taken from the 3 springs described above (figure 3). Each sampling was repeated three times. Water flow was measured on site with the volumetric

method. A WTW 320i Multi-parameter was used in situ, determining the following properties of water: pH, salinity, conductivity, redox potential, total dissolved solids. From the samples collected, were determined in the laboratory the main anions and cations, using a Dionex IC1500; the samples were filtered through a filter (0.45  $\mu\text{S cm}$ ) and diluted with ultra-pure water (18  $\text{M}\Omega\cdot\text{cm}$ ), until the sample reached a conductivity of 100  $\mu\text{S/cm}$ .

## RESULTS

### Springs's discharge

The water flow measured at the Matild spring represents only a part of the total source, namely that which is led through a pipe to a well. The captured flow of this spring is of 0.5 l/s, to which is added the flow of Drilling F 13, also 0.5 l/s. If we take into account the amount of water discharge captured and measured, at the Matild spring results a total of approx. 0.64 l/s. Compared to this value, the flows of the others are significantly lower. The discharge from Lenes is only a quarter, and that from Geza is only 12%. At all three sources, the consistency of the water flow in the four months of measurements is noticeable (table 1).

To evaluate the quantitative value of a spring, Kessler introduced in 1952 the notion of water capacity (Gribovszki et al., 2014). The higher the water flow rate, the closer the ratio between the maximum and minimum flow is closer to the unit. At the studied sources, the quantitative capacity is very good, the flow ratio being 1:1.

**Table 1.** Springs' discharge (l/s)

	<b>April</b>	<b>May</b>	<b>June</b>	<b>September</b>
<b>Matild</b>	0.13	0.14	0.14	0.14
<b>Lenes</b>	0.17	0.18	0.17	0.17
<b>Géza</b>	0.08	0.09	0.09	0.08

**Temperature.** The evolution of the spring's water temperature follows the variation of the air temperature. Thus, temperatures rise until June, and then lower values were measured in October. In all cases, the Lenes spring has the highest temperatures and Geza the lowest. The amplitudes are identical at all three sources (2°C) and are recorded between April and June (table 2).

**Table 2.** *Water temperature(°C) of the investigated springs*

	<b>April</b>	<b>May</b>	<b>June</b>	<b>September</b>
<b>Matild</b>	10.0	11.5	12.0	11.0
<b>Lenes</b>	12.0	12.5	14.0	13.0
<b>Géza</b>	9.0	10.5	11.0	10.0

**pH.** The highest values are observed at the Lenes spring, which indicates the increase of bicarbonate content, due to this Lenes spring water is a slightly basic. Here is observed the highest amplitude of values (0.6). At the Matild and Geza springs, the pH values are almost constant and close to the neutral value (table 3).

**Table 3.** *pH values of the investigated springs*

	<b>April</b>	<b>May</b>	<b>June</b>	<b>September</b>
<b>Matild</b>	7.2	7.6	7.4	7.5
<b>Lenes</b>	8.4	8.0	8.0	7.8
<b>Géza</b>	7.5	7.5	7.5	7.6

**Redox potential.** Negative values indicate the presence of reduction processes and good water quality. The lowest values are observed at the Lenes spring, and the highest at Matild. The evolution of redox potential over time is not legitimate. The maximum values are recorded in April at Matilda and Geza springs, respectively in September in Lenes (table 4). The minimums are found in April at Lenes, in May at Matilda and in September at Geza. The largest differences are at Lenes spring (29.3 mV), and the smallest at Geza (6.4 mV).

**Table 4.** *Redox potential values (mV) of the investigated springs*

	<b>April</b>	<b>May</b>	<b>June</b>	<b>September</b>
<b>Matild</b>	-24.4	-44.3	-33.8	-30.5
<b>Lenes</b>	-74.8	-59.5	-58.4	-45.5
<b>Géza</b>	-36.6	-38.2	-37.2	-43.0

**Electrical conductivity.** The high values from the Matild spring indicate a high concentration of substances dissolved in water. Due to this, the conductivity values are almost double than the normal ones (2500  $\mu\text{S}/\text{cm}$ ). At the other end is the Lenes spring, where the conductivity is very low. At all three sources the variation of electrical conductivity is relatively small (table 5). At Matild spring the values are almost constant, and the highest amplitudes are observed at Geza (1952  $\mu\text{S}/\text{cm}$ ).

**Table 5.** *Electrical Conductivity ( $\mu\text{S}/\text{cm}$ ) of the investigated springs*

	<b>April</b>	<b>May</b>	<b>June</b>	<b>September</b>
<b>Matild</b>	4550	4533	4450	4470
<b>Lenes</b>	512	613	597	575
<b>Géza</b>	3080	2740	1168	3120

**Total dissolved solids.** At the Matild spring, the concentration of dissolved solids is so high that the device used indicated "above the device limit" (OFL). This is also indicated by the very high water conductivity in this spring. The lowest values are found at the Lenes spring, where there is a remarkable consistency of concentration (amplitude only 66 mg/l). At Geza there is a remarkable parallel with the variation of electrical conductivity. At both springs, parameters' higher values appear in April and September (table 6).

**Table 6.** *Variation of the total dissolved solids (mg/l) in the investigated springs*

	<b>April</b>	<b>May</b>	<b>June</b>	<b>September</b>
<b>Matild</b>	OFL	OFL	OFL	OFL
<b>Lenes</b>	327	393	363	366
<b>Géza</b>	1970	1751	1747	1997

**Salinity.** A remarkable constancy of values is observed in the case of the Matild and Lenes springs. The difference is that in the first the values are high, the water being in the slightly salty category, and in Lenes spring the low values puts it in the sweet category (table 7). In Geza spring, the salt concentration values are average and the oscillation is significant (amplitude 1.1).

**Table 7.** *Salinity (‰) in the investigated springs*

	<b>April</b>	<b>May</b>	<b>June</b>	<b>September</b>
<b>Matild</b>	2.4	2.4	2.4	2.4
<b>Lenes</b>	0.2	0.2	0.2	0.2
<b>Géza</b>	1.6	1.4	0.5	1.6

**Cations:** Sodium ( $\text{Na}^+$ ), Calcium ( $\text{Ca}^{2+}$ ), Magnesium ( $\text{Mg}^{2+}$ ), Ammonia ( $\text{NH}_4^+$ ), Potassium ( $\text{K}^+$ ), Lithium ( $\text{Li}^+$ ).

Sodium is present in appreciable amounts in the water of the Matilda and Geza springs. The maximum concentrations are 1439 mg/l and 1111 mg/l, respectively, both in October. At these sources, the lowest quantities were measured in June (1085 mg/l and 593 mg/l). Lenes spring is characterized by very small amounts of sodium ions (between 9 - 28 mg/l).

These low concentrations significantly influence the average value, which reaches only 654 mg/l. Excluding the values from Lenes spring, the average reaches almost 1000 mg/l (see figure 4).

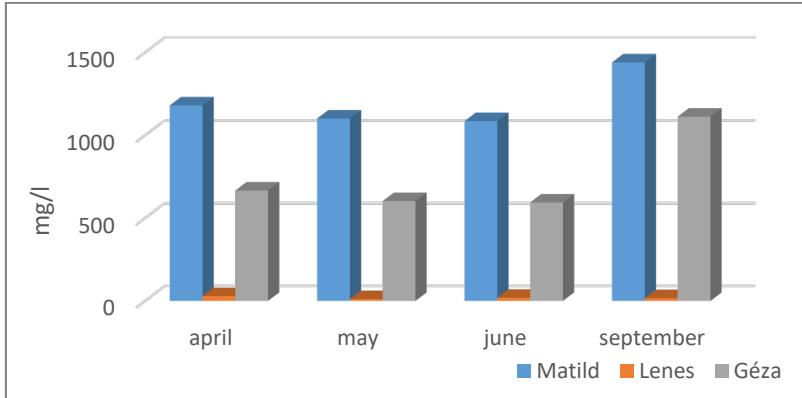


**Fig. 4.** Sodium ions variation (in the investigated months)

The concentrations of calcium are similar in all three springs. Higher values are at the Lenes spring, except in June, when the smallest quantity was measured at this spring. In April, May and October, the amount of calcium in the Matild and Geza springs is almost equal. Absolute extremes were measured at Lenes (79 mg/l in October and 52 mg/l in June). The average of all measurements is 68 mg/l and varies between 71 mg/l at Lenes and 64 mg/l at Geza (figure 5).

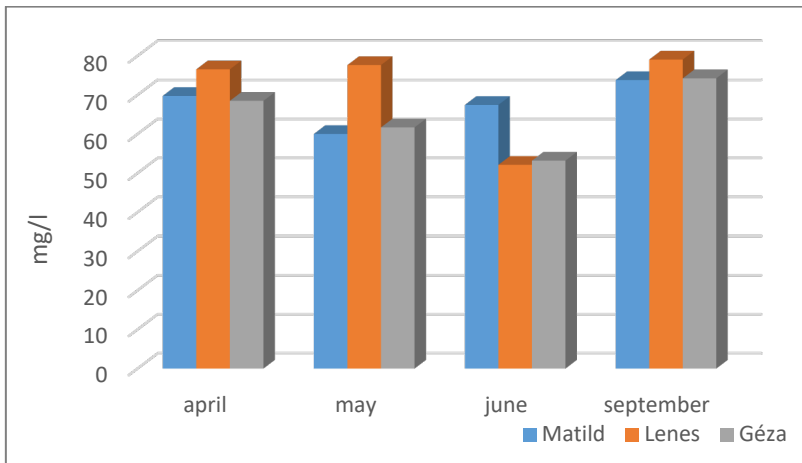


**Fig. 5.** Calcium ions variation (in the investigated months)

Magnesium has a very similar variation as sodium. In each measurement campaign, the highest values were at Matild and the lowest at Lenés. The month with maximum values at all three sources was October. The absolute maximum was recorded at Matild in October (65 mg/l), and the absolute minimum was at the Lenés spring in April (9 mg/l). The highest amplitude - 53 mg/l, was in June (64 mg/l at Matild, 11 mg/l at Lenés). The average of the measurements is 35 mg/l and varies between 54 mg/l at Matild and 13 mg/l at Lenés (figure 6).

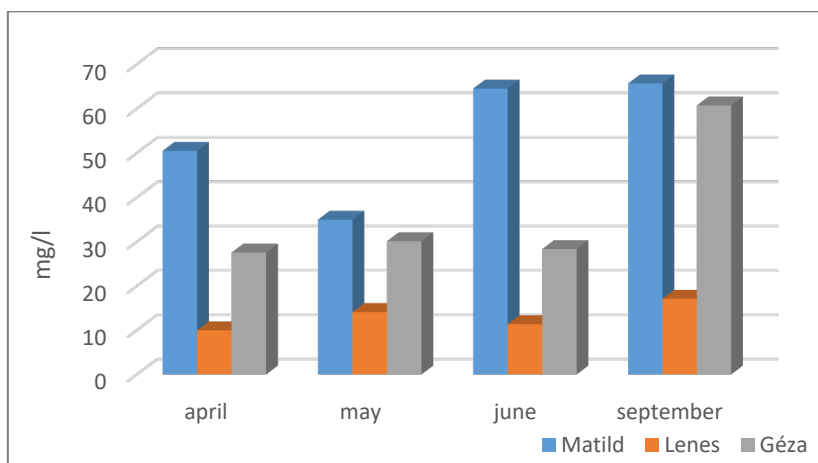


**Fig. 6.** Magnesium ions variation (in the investigated months)

Potassium was identified only at Matilda and Geza springs, in small quantities, and not in all measurement campaigns. Lithium and ammonium could not be identified at any of the three sources, with the used method.

**Anions:** Fluorides ( $F^-$ ), Chlorides ( $Cl^-$ ), Bromides ( $Br^-$ ), Nitrites ( $NO_2^-$ ), Nitrates ( $NO_3^-$ ), Phosphates ( $PO_4^{3-}$ ), Sulphates ( $SO_4^{2-}$ ), Bicarbonates ( $HCO_3^-$ ).

Fluorides registered very high values in April, at the Matild and Geza springs (1.80 mg/l, respectively 1.75 mg/l), which exceeds the limit of 1.2 mg/l according Law no 311/2004, for drinking water in Romania. Otherwise, the values were below 1 mg/l at all sources. The Lenés spring values varied the most, between 0.35 mg/l in May and 0.28 mg/l in October. The absolute minimum value (0.23 mg/l) was at Matild in May. The measurements' average is 0.75 mg/l. The maximum average of 1.01 mg/l was recorded at the Geza spring, and the minimum average at Lenés (0.32 mg/l) (figure 7).

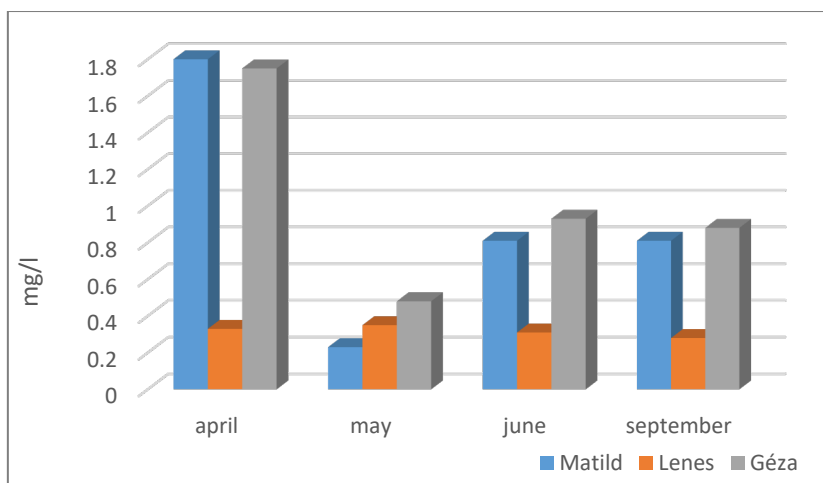


**Fig. 7.** Fluorides variation (in the investigated months)

The variation of chlorides concentration closely follows that of sodium. That is, in the water of the Matild and Geza springs there are much larger quantities than at Lenés. The chloride in the Matild spring is relatively constant, very close to 400 mg/l, in all four months of measurements. This relative constancy is maintained also at the Geza spring, but with lower values (between 143 and 220 mg/l). At Lenés, the chlorides do not exceed 25 mg/l. The amplitude of the extreme values is very high: maximum 427 mg/l at Matild and 14 mg/l at Lenés. The average of all measurements is 200 mg/l (figure 8). The maximum concentration given by 311/2004 law for drinking waters is 250 mg/l.

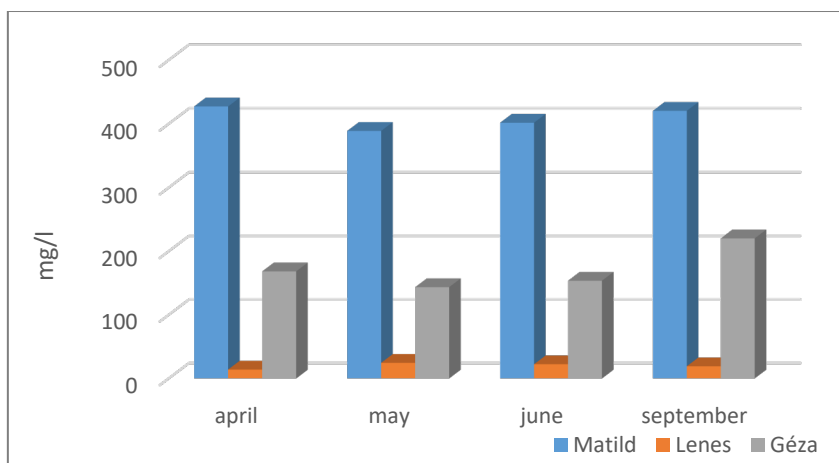


**Fig. 8.** Chlorides variation (in the investigated months)

Nitrates are present in relatively similar quantities at all three springs. Slightly higher values were measured at the Lenes spring. Here is the maximum recorded value of almost 20 mg/l in May. The minimum value, just over 13 mg/l, was registered at the Matild spring in April and October, as well as at the Geza spring in the first three months of measurements. The average nitrate concentration is 15.5 mg/l (figure 9).

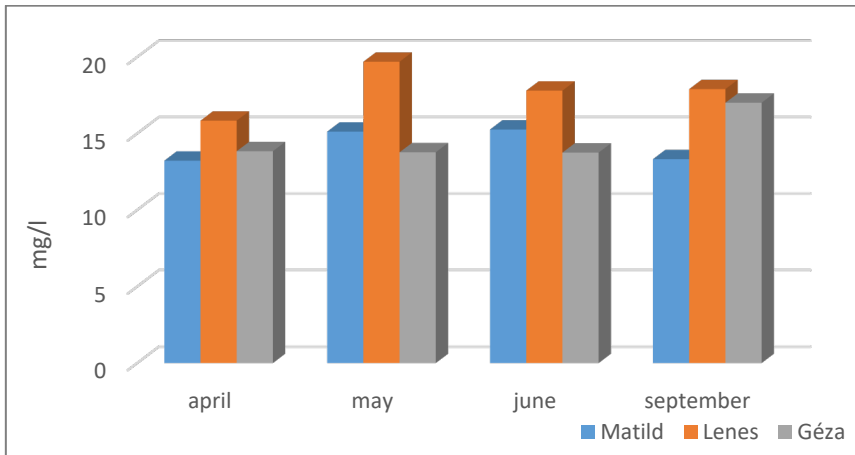


**Fig. 9.** Nitrates variation (in the investigated months)

Sulphates have values above 11 mg/l at the Lenes spring at all measurements and at Geza in June. The maximum of 13 mg/l is at the Lenes spring in June. The concentration in the Matild spring is very constant, with an amplitude of only 0.48 mg/l. The minimum value was measured at the Geza spring in April - 6.5 mg/l. The average of sulphate values is almost 10 mg/l (figure 10).

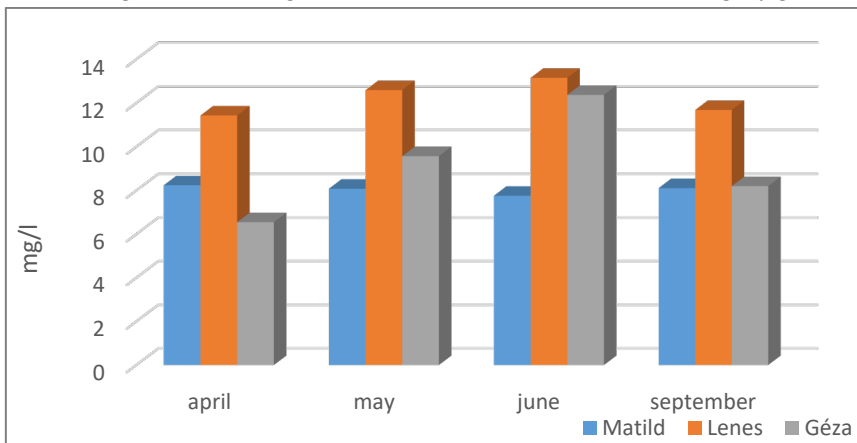


**Fig. 10.** Sulfate variation (in the investigated months)

The concentration of bicarbonates is appreciable at all sources (over 1000 mg/l). Constantly high values, over 1600 mg/l, were measured at Matild. The water from Lenes (640 mg/l) and Geza (415 mg/l) springs has higher amplitudes. The highest value was recorded at Matild in October (1675 mg/l) and the lowest at Lenes in April (1040 mg/l). The average concentration is 1441 mg/l (figure 11).

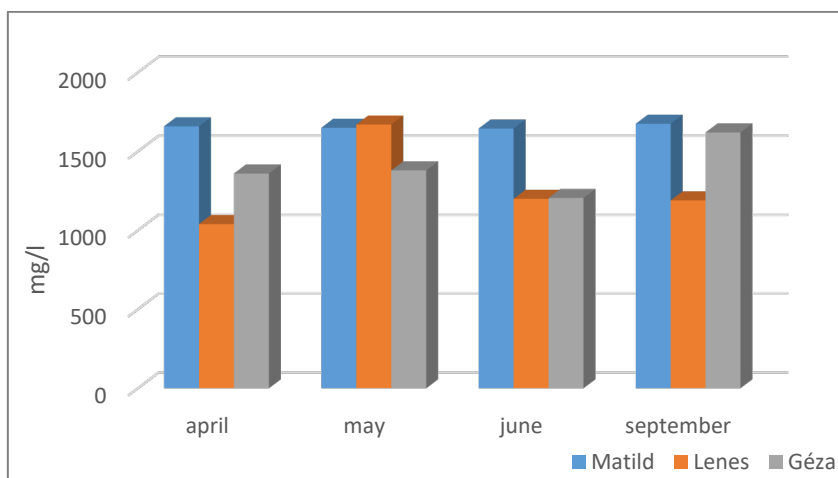


**Fig. 11.** Bicarbonate variation (in the investigated months)

Bromides, nitrites and phosphates could not be identified by the used method on Dionex Ion Chromatograph.

## CONCLUSIONS

The mineral waters of Bodoc, currently insufficiently exploited, are an important source, both for food and spa tourism. The physical properties of these waters and their chemical composition indicate a remarkable variety and qualities that must be exploited.

The main source is Matild, which is bottled. There is a remarkable balance in terms of water flow temperature and pH. The concentration of salts and dissolved substances is high. Among cations, sodium dominates with values above 1000 mg/l, calcium and magnesium having values below 100 mg/l. The most important anions are bicarbonates (over 1500 mg/l) and chlorine (around 400 mg/l). These indicators, together with the other components, give Bodoc waters a carbonate – sodium - alkaline characteristic.

Munteanu C. states that alkaline mineral waters are in the form of combinations (chlorine-sodium, carbonated, sulphurous, sulphated, ferruginous, etc.) and joins the waters of Bodoc to those of Sângeorz, Hebe, Slănic Moldova, Malnaş, Karlovy Vary (Munteanu, 2013).

The National Mineral Waters Company through the Exploitation License no. 54/1999 defines the water from the Bodoc perimeter as natural hydrogen-carbonated-sodium mineral water.

Regarding the spa tourism value of these waters, they are recommended for internal cures and aerosols (Teodorescu and Gaceu, 2013).

## REFERENCES

- Airinei St., Pricăjan A., 1972, Corelații între structura geologică profundă și aureola mofetică din Județul Covasna cu privire la zonele de apariție a apelor minerale carbogazoase. *Aluta*, Sf. Gheorghe, pp. 181-193.
- Bandrabur T., Slăvoacă D., 1973, Apele minerale din zona Malnaş – Ozunca. *Studii de hidrogeologie*, București.
- Feru A., 2012, Ghidul apelor minerale naturale. Risoprint, Cluj-Napoca.
- Gribovszki Z., Kalicz P., Kucsara M., 2014, Víztan, West Hungarian University. Sopron, 240 p.
- Kisgyörgy Z., Dukrét L., 2001, Baróti-hegység, Bodoki-havasok. Pallas Publishing, Miercurea Ciuc.
- Kisgyörgy Z., 2008, Amiből Mátyás király is ivott. *Háromszék daily newspaper*, Sepsiszentgyörgy.
- Hankó V., 1887, Bodoki hideg savanyúvíz elemzése. *Mathematics and Science Bulletin*, M.T.A., Budapest.
- Harkó J., 1970, A Málnási és Bodoki borvizek monográfiája. *Tanulmány*.
- Munteanu C., 2013, Apele minerale terapeutice, Balneară Publishing, Bucharest.
- Orbán B., 1982, republication, A Székelyföld leírása I, II. Helikon Publishing, Budapest.
- Teodorescu E., Gaceu O., 2013, Turism balnear în România. Oradea Universității Publishing, Oradea.
- \*\*\* The National Society of Mineral Waters, 1999, Exploitation license no. 54/1999.